REPORT DOCUMENTATION PAGE Dist: A

Form Approved
OMB No. 0704-0188

Public reporting burden for this collection of information is estimated to average 1 hour per response, including the time for reviewing instructions, searching existing data sources, gathering and maintaining the data needed, and completing and reviewing the collection of information. Send comments regarding this burden estimate or any other aspect of this collection of information, including suggestions for reducing this burden, to Washington Headquarters Services, Directorate for Information Operations and Reports, 1215 Jefferson Davis Highway, Suite 1204, Arlington, VA 22202-4302, and to the Office of Management and Budget, Paperwork Reduction Project (0704-0188), Washington, DC 20503.

1. AGENCY USE ONLY (Leave blank)	2. REPORT DATE	3. REPORT TYPE AND DATES COVERED
	29 Nov. 94	Final Report 30, Sept. 91-Sept. 94 29,

4. TITLE AND SUBTITLE
Origins of Imperfections in Composite Materials

5. FUNDING NUMBERS
AFOSR Grant-91-0437
2302/DS

6. AUTHOR(S)
Robert E. Green, Jr.

7. PERFORMING ORGANIZATION NAME(S) AND ADDRESS(ES)
Center for Condestructive Evaluation
The Johns Hopkins University
3400 N. Charles St.
Baltimore, MD 21218-2689

8. PERFORMING ORGANIZATION REPORT NUMBER
AFOSR-TR- 95 0050

9. SPONSORING/MONITORING AGENCY NAME(S) AND ADDRESS(ES)
AFOSR/NA
110 Duncan Avenue, Suite B115
Bolling AFB, DC 20332-0001
NA

10. SPONSORING/MONITORING AGENCY REPORT NUMBER
AFOSR-91-0437

11. SUPPLEMENTARY NOTES

19950127 083

DTIC ELECTE JAN 31 1995 S D

12a. DISTRIBUTION/AVAILABILITY STATEMENT
Approved for public release, distribution unlimited

Original contains color plates: All DTIC reproductions will be in black and white.

12b. DISTRIBUTION CODE
B
A

13. ABSTRACT (Maximum 200 words)

This research applied advanced ultrasonic techniques for detection of the origin of imperfections in composite materials used in aircraft and aerospace structures. Previous work supported by the U.S. Air Force Office of Scientific Research showed that ultrasonic attenuation monitoring proved to be superior to other nondestructive evaluation techniques for detection of early fatigue damage in aluminum alloys used in aircraft construction. In addition ultrasonics is the only technique which affords the possibility of detecting defects from one side of the material. In order to detect microscopic defects, an additional aspect of this work was to optimize acoustic microscopy techniques for detection of the origin of very small imperfections. Included in the techniques used were air-coupled ultrasound to detect the quality of composite prepregs. Because ultrasonic techniques are not capable of measuring residual stress in composite materials a novel micro-photoelastic system was developed for measurement of residual stress in optically translucent ceramic matrix composites. However, ultrasonics could detect manufacturing flaws and micro-porosity in ceramic composites. The overall goal was to identify the origin of imperfections in composite materials used in aircraft and aerospace structures and to optimize ultrasonic nondestructive evaluation techniques for detecting these imperfections.

14. SUBJECT TERMS
DTIC QUALITY INSPECTED 3
graphite-epoxy, ceramic matrix, metal matrix, composites, defects, ultrasonics, acoustic microscopy, air-coupled ultrasound, residual stress, micro-photoelasticity

15. NUMBER OF PAGES
53

16. PRICE CODE

17. SECURITY CLASSIFICATION OF REPORT	18. SECURITY CLASSIFICATION OF THIS PAGE	19. SECURITY CLASSIFICATION OF ABSTRACT	20. LIMITATION OF ABSTRACT
UNCLASSIFIED	UNCLASSIFIED	UNCLASSIFIED	UL

Acknowledgements

The author would like to acknowledge his graduate students who contributed to the success of this research effort: Chris Byrne who performed most of the experimental research effort; Tobias Berndt for performing the air-coupled ultrasound images; Joe Krynicki for his development and application of the micro-photoelastic technique. Thanks are due Walter Krug and Mike Franckowiak for their outstanding work in machining specimens and components and to Ms. Debby Manley for assistance in manuscript preparation.

Thanks are also due the Naval Surface Warfare Laboratory, Annapolis Detachment for allowing graphite-epoxy specimens to be manufactured in their facilities, to Dr. Dennis Nagle formerly of the Martin Marietta Research Laboratories for the ceramic composite specimens, and to Dr. John Liu of the Naval Surface Warfare Laboratory, White Oak for supplying the metal matrix composite specimen. He is grateful for the financial support and understanding of difficulties encountered in the first two years research effort. In this regard special thanks are due Dr. Jim Chang, Dr. Walter Jones, and Dr. Spencer Wu, AFOSR/NA.

DISCLAIMER NOTICE

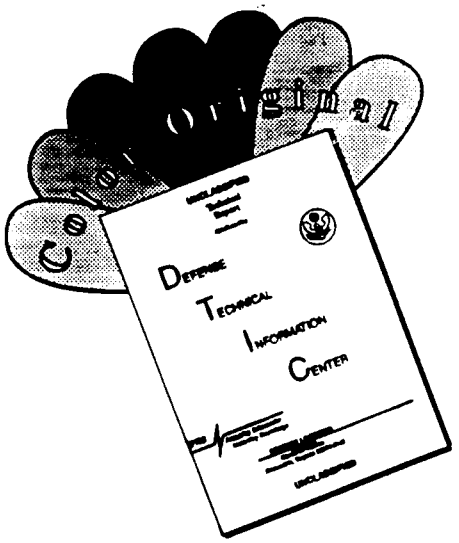

THIS DOCUMENT IS BEST QUALITY AVAILABLE. THE COPY FURNISHED TO DTIC CONTAINED A SIGNIFICANT NUMBER OF COLOR PAGES WHICH DO NOT REPRODUCE LEGIBLY ON BLACK AND WHITE MICROFICHE.

Origins of Imperfections in Composite Materials

Robert E. Green, Jr.
Center for Nondestructive Evaluation
The Johns Hopkins University
Baltimore, MD 21218-2689

Executive Summary

Increasingly composite materials are replacing metal components in aircraft and aerospace structures. These composite materials will be required to exhibit superior performance to metals in ever more demanding stressful situations. In addition, since they will be subjected to severe fatigue loading, it is imperative that optimum nondestructive evaluation techniques be developed for detection of the origin of imperfections in these composite materials.

The research supported by this AFOSR grant applied advanced ultrasonic techniques for detection of the origin of imperfections in composite materials used in aircraft and aerospace structures. Previous work supported by the U.S. Air Force Office of Scientific Research showed that ultrasonic attenuation monitoring proved to be superior to other nondestructive evaluation techniques for detection of early fatigue damage in aluminum alloys used in aircraft construction. In addition ultrasonics is the only technique which affords the possibility of detecting defects from one side of the material. In order to detect microscopic defects, an additional aspect of this work was to optimize acoustic microscopy techniques for detection of the origin of very small imperfections. Included in the techniques used were air-coupled ultrasound to detect the quality of composite prepregs. Because ultrasonic techniques are not capable of measuring residual stress in composite materials a novel micro-photoelastic system was developed for measurement of residual stress in optically translucent ceramic matrix composites. However, ultrasonics could detect manufacturing flaws and micro-porosity in ceramic composites. The overall goal was to identify the origin of imperfections in composite materials used in aircraft and aerospace structures and to optimize ultrasonic nondestructive evaluation techniques for detecting these imperfections.

DTIC QUALITY INSPECTED 3

Introduction

The term composite covers a wide variety of materials, including boron/epoxy, glass/epoxy, graphite/epoxy, graphite/peek, Kevlar/epoxy, silicon carbide fiber reinforced silicon carbide matrix, carbon/carbon and metal matrix. Nondestructive evaluation of composite materials is appreciably more complex than nondestructive evaluation of monolithic metals and ceramics primarily because of the types of imperfections causing failure of each material. In metallic and ceramic materials the predominant failure causing flaws are cracks and those imperfections which may lead to crack initiation and growth.

In any discussion of imperfections in composites materials and their detection or characterization through nondestructive evaluation, one needs to set ground rules concerning the kind and size of the imperfections, the point in the processing or life cycle of the material where the imperfections occur, and the nature of the NDE method to be employed. In some cases, methods are well known and widely used, but of limited capability. Broadly speaking, imperfections in continuous fiber composites may be separated into two main categories. There are manufacturing imperfections -- induced during fabrication -- and in-service imperfections -- arising from damage or degradation of the composite while exposed to its working environment.

Manufacturing imperfections include processing defects like delaminations, misorientation of fibers, resin-rich or resin-poor regions, incomplete cure of the matrix or incorrect cure cycle leading to trapped gas porosity, or large voids. Better control of the fabrication process using information developed through real-time nondestructive sensing could reduce or eliminate many of these problems. Protective backing paper on the pre-preg material is sometimes not removed and cures into the laminate. The result is a reduction of the shear strength of the finished composite nearly to zero in the region of the foreign matter. Manufacturing variances generally result in changes in the properties of the composite, some of them potentially serious. Depending on the application one type or class of imperfection may be more diligently sought than another.

During usage, discrete damage to the composite may occur from the impact of objects, hammers, wrenches or other tools on the laminate surface. The impact initiates a shock wave that propagates away from the impacted surface and causes its largest effect, because of total reflection, near the far surface. Characteristically, the impact-induced delamination will grow with depth into the laminate. In-service induced fatigue damage is another source of extreme imperfections in composite aerospace structures. Water absorption can also be a serious in-service problem for some

☑ ☐ ☐

Availability Codes
Dist | Avail and/or Special
A-1

types of matrix resins, where elevated moisture content leads to plasticizing of the matrix and can change the stress state to favor cracking. Less important environmental mechanisms are photo or thermal oxidation, radiation damage, hydrolytic degradation, or electrochemical corrosion.

Listed below are various composite imperfections and some estimates of sizes that can reliably be found with current field NDE practice or with techniques under development in research laboratories. However, a caveat is in order here. While widely sought in the industrial environment, minimum detectable NDE size estimates are numbers to be handled with caution. They are almost always misleading. Extensive data on NDE reliability gathered in government sponsored programs in several NATO countries over two decades consistently demonstrate that there is no flaw too large to be missed by some inspectors on some occasions using some methods. Therefore, the NDE size estimates offered here are only very rough numbers and, like any such guess, must be predicated on reasonable assumptions. They are intended as quantitative limits -- some NDE may perform better, some worse -- and cannot be warranted to be achievable by all, or even most, current inspectors.

Degree of Cure

Thermoset resins often require knowledge of the degree of cure to assure the product user that the properties assumed in the design of the component are indeed the ones in any particular example. Most efficient is the continuous monitoring of the composite during cure, where changes can be made to compensate for cure variations. Research in this area has centered on ultrasonic wave or mechanical damping and ultraviolet fluorescence. However, in conventional practice one monitors the external process variables, such as temperature and pressure, in order to control the rate of cure. More detailed nondestructive information about the precise cure state of the material is highly desirable.

Fiber Orientation

In thick laminates intended for structural applications, lamina are usually composed of many individual plies. Each lamina may contain 10 to 30 plies, stacked in a sequence to form a laminate from 3 to 12 inches thick. It is of interest to users of these laminates to assure nondestructively that the correct stacking sequence has been followed. This is because the stacking sequence will substantially determine the tailored stiffness of the finished product. Currently, manufacturers use careful paperwork checks during layup to assure the proper sequence.

Fiber Volume Fraction

Since the mechanical characteristics of composites stem largely from the fibers, the fiber-matrix ratio is a useful measure of quality. Composite fiber volume fraction must not be either too large or too small. On the other hand, the composite derives its stiffness and strength largely from the fibers, with the matrix acting principally as a load-transfer medium. So, fiber volume fraction must be high enough to insure the specified properties. However, at typical fiber volume fractions of 0.60 to 0.68 in graphite-epoxy one is not too far from serviceable packing fraction limits (The maximum theoretical fiber volume is 90%). Therefore, it is necessary to determine that there are no resin-poor regions in critical areas of the structure. Without sufficient resin complete wetting cannot occur, degrading the mechanical properties. Fiber fraction can be determined by ultrasonic wavespeed, provided other certain conditions are taken as given. These include the elastic moduli of the constituents, ply, layer, and laminate thickness and the geometry of the layup. Industrial systems exist to make such measurements on the uncured pre-preg. After cure, manufacturers usually rely on conventional ultrasonic c-scanning to reveal areas of low or high resin content. The smallest such defect that can be reliably found would depend on the location in the laminate and the sensitivity of the nondestructive inspection as performed by the fabricator. Generally, 1/2 square inch defects can be found, but 1/8 square inch defects cannot.

Porosity

Gasses of volatile organics evolved during cure of the composite can be trapped in the laminate if the rate of cure is improperly chosen for the type and thickness of the composite. The resulting porosity is a serious strength-limiting defect above a volume fraction of 2 or 3 % in most matrix systems. In current practice, ultrasonic attenuation is usually employed to assess the severity of gas porosity by comparing standard specimens with known porosity levels to products taken out of the autoclave. Sensitivity of 1/2 % is desired.

Fiber/Matrix Bonding

Wetting at the fiber/matrix interface is the problem here. This topic is closely related to the previous one, so long as one restricts consideration to wetting due to fiber fraction or fiber dispersion. Generally, this property is dominated by the quality of the pre-preg, and might be better tested for at that stage in the fabrication. Microscopic bonding at the fiber/matrix interface is much more difficult to assess nondestructively.

Interfacial Bonding

Good interfacial bonding is required to insure proper transfer of shear loads at the interfaces between successive plies or between successive lamina. Bond integrity is a particularly difficult problem for NDE, since by definition one normally measures mechanical properties in the linear elastic regime (to avoid damage to the material), while failure of the bond is an essentially nonlinear phenomenon. To begin to see how to nondestructively assess bond quality one must consider which bond-related effects are reliably correlated with properties or characteristics accessible to NDE. Alternatively, one could imagine stressing the bond until some nonlinear behavior is induced.

Ultrasonic Waves in Solid Materials

Ultrasonic techniques have been used much more than any other nondestructive method to investigate composite materials. Among these ultrasonic techniques pulse-echo or pulse-transmission procedures have been used most often in the conventional contact, water immersion or water squirter modes to measure velocity and attenuation and thereby determine the associated mechanical properties. These techniques have been used to detect voids, inclusions, disbonds, cracks, delaminations, cure, lay-up order, fatigue life, fiber orientation, residual strength, and resin-starved areas. However, the use of ultrasonic waves as nondestructive probes has as a prerequisite the careful documentation of the propagational characteristics of the ultrasonic waves themselves. Since in nondestructive evaluation applications it is not desirable for the ultrasonic waves to alter the material through which they pass, it is necessary to work with very low amplitude waves, which normally are regarded to obey linear elasticity theory. Although most practical uses of ultrasonics are applied to solid materials which are polycrystalline aggregates and therefore assumed to be isotropic, with real crystalline solids and composites the condition of ideal isotropy is extremely difficult, if not impossible, to attain.

Linear Elastic Wave Propagation

In general three different linear elastic waves may propagate along any given direction in an anisotropic material. These three waves are usually not pure modes since each wave generally has particle displacement components both parallel and perpendicular to the wave normal. However, one of these components is usually much larger than the other; the wave with a large parallel component is called quasi-longitudinal while the waves with a large perpendicular component are called quasi-shear. In the event that the material is isotropic, then all modes

become pure modes, i.e. the particle displacements are either parallel or perpendicular to the wave normal, and the two quasi-shear modes degenerate into one pure shear mode. Also of great practical importance to elastic wave propagation in anisotropic materials is the fact that the direction of the flow of energy per unit time per unit area, the energy-flux vector, does not in general coincide with the wave normal as it does in the isotropic case, i.e. the ultrasonic beam exhibits refraction even for normal incidence.

Attenuation of Nearly Linear Elastic Waves

For all real solids, the assumption of pure linear elasticity is only an approximation, since all real ultrasonic waves are attenuated as they propagate. If one considers this more realistic case, one finds, to the lowest order of approximation, that the general propagational characteristics of such waves in solid materials are identical with the linear elastic case as regards wave speeds, particle displacements, energy flux vectors, and diffraction spread. However, as a result of various mechanisms, there will be energy loss from these waves.

Although geometrical effects can cause energy to be lost from the ultrasonic beam, such losses are not indicative of intrinsic loss mechanisms associated with the microstructure. Once proper precautions are taken to either eliminate or control these geometrical effects, ultrasonic attenuation measurements serve as a very sensitive indicator of internal loss mechanisms caused by microstructures and microstructural alterations in the material. This sensitivity derives from the ability of ultrasonic waves of the appropriate frequency to interact with a variety of defects including cracks, foreign particles, precipitates, porosity, fiber breaks, delaminations, disbonds, voids, grain boundaries, interphase boundaries, and dislocations.

Nonlinear Elastic Wave Propagation

Nonlinear effects associated with ultrasonic wave propagation may also be used to advantage for nondestructive materials characterization. Nonlinear effects in elastic wave propagation may arise from several different causes. First, the amplitude of the elastic wave may be sufficiently large so that finite strains arise. Second, a material, which in its undeformed state behaves in a linear fashion, may behave in a nonlinear fashion when infinitesimal ultrasonic waves are propagated, provided that a sufficient amount of external static stress or internal residual stress is superimposed. Finally, the material itself may contain various energy absorbing mechanisms such that it is locally nonlinear, e.g. the defects enumerated previously.

Nonlinear elastic waves differ from linear elastic waves in several important aspects. An initially sinusoidal nonlinear longitudinal elastic wave of a given frequency distorts as it propagates, and energy is transferred from the fundamental to the harmonics that appear. The degree of distortion and harmonic generation is directly dependent on the amplitude of the wave. A pure mode nonlinear longitudinal wave may propagate alone, but a pure mode nonlinear transverse wave cannot propagate without the existence of an accompanying longitudinal wave. On the other hand, a nonlinear transverse wave does not distort when it propagates in a defect free solid. Nonlinear elastic waves can interact with other waves in the solid. At the intersection of two ultrasonic beams, additional ultrasonic beams can be generated. Interaction with thermal vibrations causes energy loss from the wave. The degree of interaction in all cases is directly dependent on the amplitude of the wave.

Ultrasonic Waves in Inhomogeneous Materials

Additional problems arise with ultrasonic wave propagation in inhomogeneous materials. The presence of a single bounding surface complicates the propagational characteristics of ultrasonic waves in solid materials and can lead to erroneous interpretation of velocity and attenuation measurements. The presence of many bounding surfaces, such as occur in composites, complicates the propagational characteristics even more and, except in a few special cases, the problems have not been solved analytically. However, solution of these problems will permit proper ultrasonic measurements to be an invaluable tool in characterizing composite materials. The present research has contributed considerably to these solutions.

Materials

Material selection was determined by availability from manufacturers, from both government and industrial research laboratories, and by the ability to manufacture composite specimens at local government and industrial laboratories and the Johns Hopkins University Applied Physics Laboratory. Among the materials investigated were graphite-epoxy, metal matrix, and ceramic matrix composites. Most tests were conducted on graphite-epoxy composites because these are currently the composites most often used in the aircraft and aerospace industries. Graphite-epoxy composite specimens were tested as prepregs, thin plates, and thick plates. The graphite-epoxy composite specimens were made using continuous graphite fibers in a (Hercules AS4/3501-6) epoxy polymer matrix. The metal matrix composite was made from continuous graphite fibers in an aluminum matrix and only few tests were performed on this composite because of difficulty of obtaining specimens. The ceramic matrix

composites were fabricated from a 7740 borosilicate glass with either a Nicalon silicon carbide single tow or woven cloth as the reinforcement. While other matrices were considered and tried, the 7740-type best suited the thermomechanical compatibility criteria. The three important features of the glass were: (1) Its coefficient of thermal expansion is relatively close to that of the Nicalon fiber and, therefore, minimizes processing stresses. (2) It is relatively inexpensive and is, therefore, an economically attractive composite constituent. (3) It is optically transparent thereby making the ceramic matrix composite eligible for photoelastic stress analysis. Some specimens were nondestructively inspected in the as-fabricated state, while others were inspected after quasi-static or fatigue testing.

Mechanical Tests

Two MTS compression testing machines incorporating fixtures for uniaxial fatigue tensile or compression testing of composite materials were used for on-line computer control of testing protocol and data acquisition. Tensile tests were conducted on specimens following ASTM protocal. Both Quasi-static and Compression-compression fatigue tests were conducted on 1 inch square cross-section, 3 inch long graphite/epoxy composite specimens many of which possessed stress (strain) concentrators. Unique grips were designed for these specimens and successfully shown to load the specimens without "brooming". Quasi-static compression data was obtained to characterize the material and the results compared with those of other investigators. Fatigue tests established the S/N curve for catastrophic failure. Subsequent fatigue tests were run at loads well below the failure loads to provide specimens with appropriate lesser damage, which in turn was the focus of various on-line and off-line nondestructive monitoring techniques.

Detection of Prepreg Defects
(Fiber misalignment, Porosity)

The initial tests conducted on prepregs were water-coupled ultrasonic c-scan in order to determine the uniformity of fiber alignment and distribution of polymer resin throughout the prepreg. Although this technique yielded excellent images of the non-uniformity of prepreg over the entire area of the test specimens, the requirement to immerse the specimens in water rendered the prepregs useless for fabrication of composites. Therefore, both for prepreg process control applications and for quality control of prepreg materials for composite fabrication a non-contact air-coupled ultrasound c-scan system was developed to inspect prepreg thus eliminating the necessity of immersing the prepreg in water. The system proved capable of transmitting ultrasound through the prepreg in a

transmission mode in air at ambient room temperature and pressure.

Historically, one obstacle to the use of air-coupled ultrasound was the misconception that the absorption in air was excessively high, while actually it is only 20 dB/m at 600kHz and 20 degrees Centigrade. The signal-to-noise performance of an ultrasound system is best when there is a small difference in acoustic impedance (product of density and wave speed) between the materials through which the ultrasonic wave passes. For the conventional water-coupled or other liquid-coupled systems, the impedance mismatch between the liquid and solid is small compared to the mismatch between air and solid, since the acoustic impedance of most solids is four or five orders of magnitude larger than that of air. As a result, the signal-to-noise ratio for liquid-coupled systems is typically sixteen orders of magnitude higher than that in air-coupled systems and explains why conventional ultrasound using liquids is much easier and, therefore, more common than air-coupled ultrasound.

However, modern technology now permits overcoming the low signal-to-noise ratio associated with air-coupled ultrasound by judicious selection of critical components of the air-coupled ultrasound system. The transducers used were piezoelectric thickness-mode transducers operated at 500 kHz. They were selected because they provided good signal-to-noise performance at this frequency. **Figure 1** shows a schematic diagram of the air-coupled ultrasound system used in the present research. The system was digitally controlled and consisted of a Ritec Advanced Measurement System, RAM 10000, which generated and processed the ultrasonic signals. It was linked to a commercial Sonix c-scan system, which controlled the position of the transducers in the x-y plane. A computer containing a 12-bit analog to digital converter controlled the measurement and scanning systems and stored data for the amplitude, phase, x and y positions, and the measurement system settings. The system operated between 50 kHz and 5 MHz. The RAM phase-sensitive superheterodyne measurement system had modules that contained different components including: an IF oscillator and quadrature phase sensitive detectors, a direct digital synthesizer, a high power gated RF amplifier, a broadband RF receiver, a mixer and IF amplifier, a gated analog integrator, and a coherent timing component.

A detailed view of the transducer/specimen configuration is shown in **Figure 2**. The transducers were mounted on rods that had 360 degrees rotation around the vertical axis, could be positioned at any distance from each other within 20 cm, and could be locked into position along a horizontal beam. The beam could also be rotated 360 degrees. This configuration was designed to permit scanning

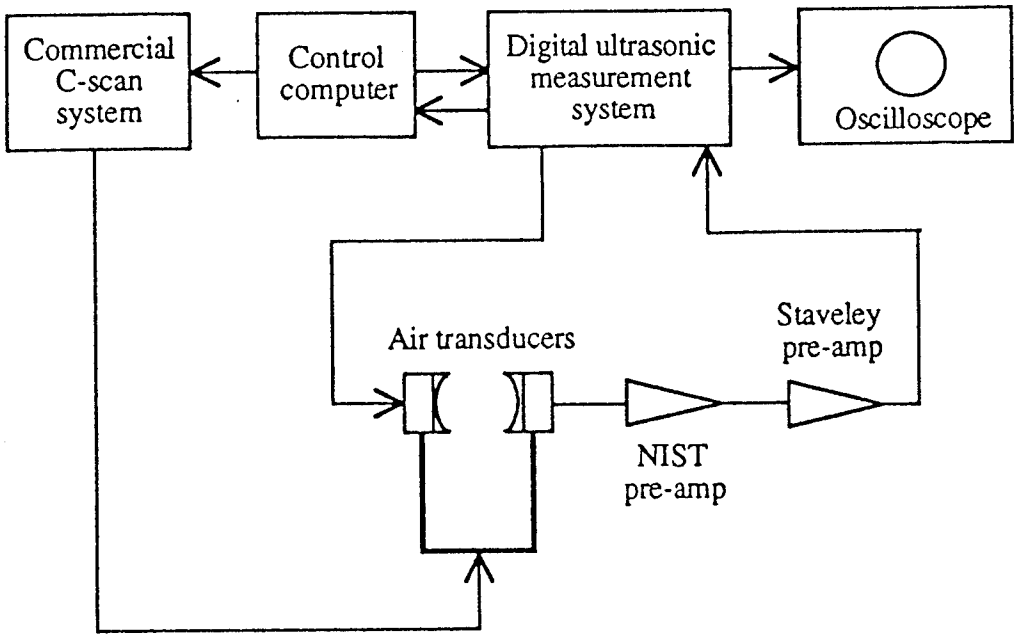

Figure 1. Schematic diagram of air-coupled ultrasound system.

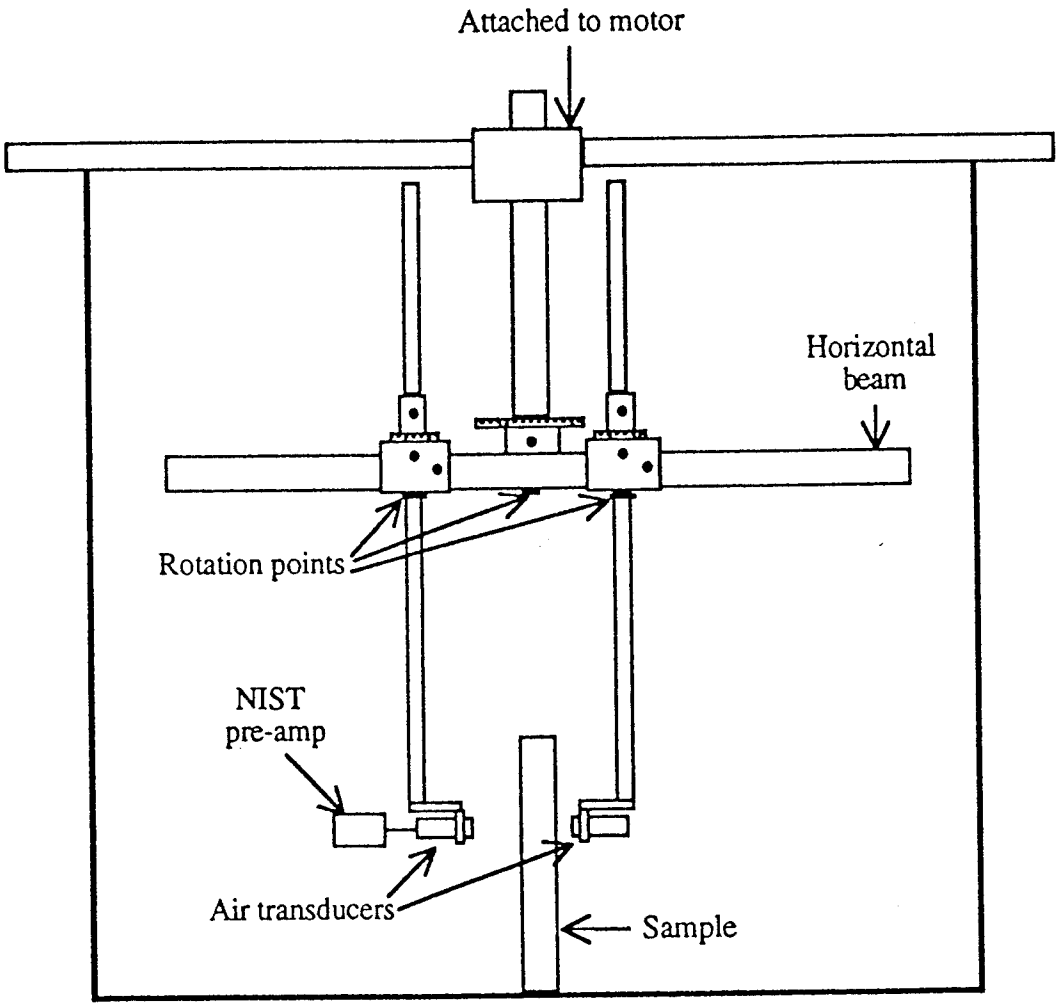

Figure 2. Detailed view of air-coupled ultrasound transducer/specimen configuration.

with transducers at different distances from each other and at different angles with respect to each other. The entire transducer support system was attached to the motorized c-scan computer controlled system. During the scans, the generating transducer was positioned 1 cm and unfocused on one surface of the prepreg. The receiving transducer was positioned 5 cm from the opposite surface of the prepreg and focused on the prepreg-air interface. This configuration insured that the maximum energy entered the prepreg and provided the highest resolution images.

Figure 3 shows the c-scan amplitude image of a graphite-epoxy prepreg obtained with the air-coupled ultrasound system, while **Figure 4** shows the c-scan phase image of the same specimen. Both figures clearly serve to show resin rich and resin poor regions throughout the area of the specimen.

Residual Stress (Strain) Measurement

While an important property in composites, as in metals, residual stress (strain) has historically been difficult if not impossible to measure. Typically, in crystalline materials such as monolithic ceramics and metals one seeks to measure stress by observing the changes it induces in atomic lattice constants, either through x-ray diffraction or variations in ultrasound velocity. In composites, the ultrasonic measurement is further complicated by the fibers, whose presence introduces uncertainties in ultrasonic data, similar to the effect of texture in polycrystalline metals. Moreover, since the fibers are so much stiffer than the matrix (typically a factor of 40 or more in the axial direction), most of the deformation is concentrated in the polymer matrix. This is an important, but an unsolved challenging problem.

Because ultrasonic techniques are not capable of measuring residual stress in composite materials a novel micro-photoelastic system was developed for measurement of residual stress in optically translucent ceramic matrix composites. The use of reinforcing fibers for ceramic matrix composites is drastically different from that of polymer or metal based systems. For the latter two, it is desired that an extremely strong and perfect bond exists between the matrix and reinforcement. By having a perfect bond and consequently excellent fiber-matrix adhesion, complete load transfer between the fiber and matrix can occur, thereby enhancing the mechanical properties of the usually less stiff and/or weaker matrix. Contrary to this idea, ceramic matrices are already stiff and have high theoretical strengths; their nemesis is toughness. The failure strain of most ceramics is usually substantially less than that of the reinforcement. This scenario is the inverse case of polymer or metal based systems. In this

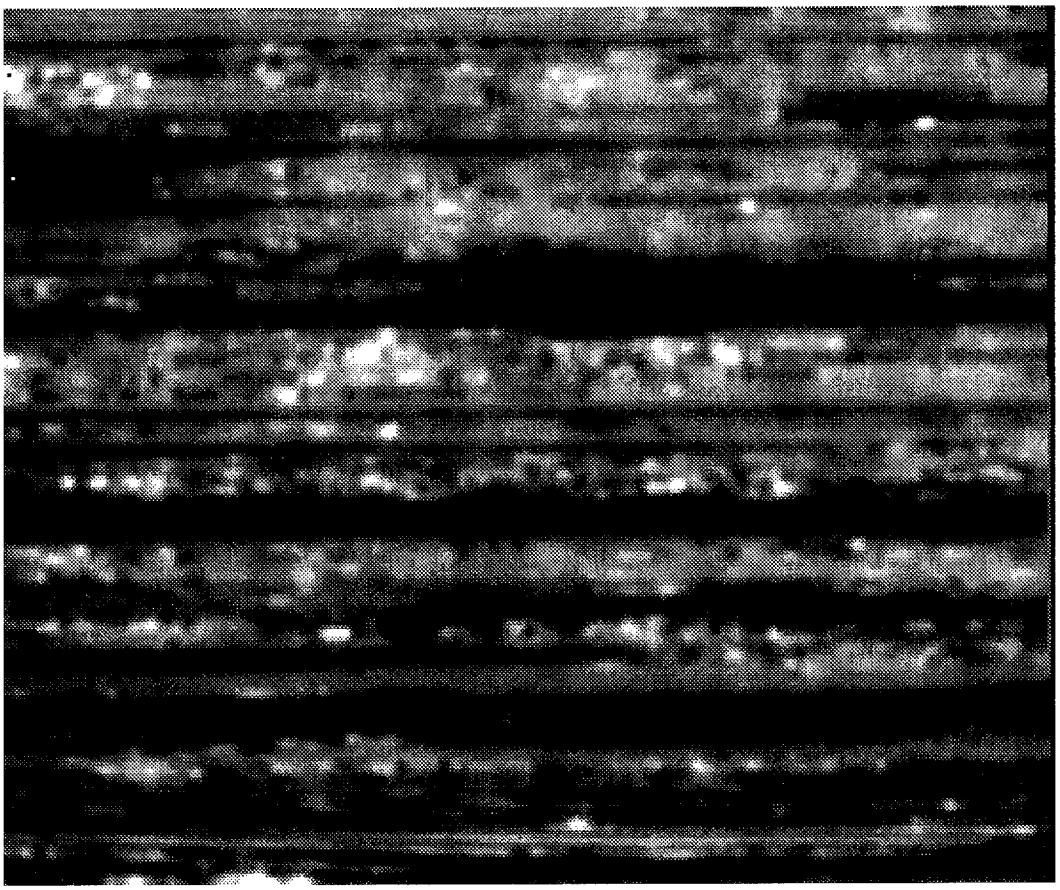

Figure 3. C-scan amplitude image of graphite-epoxy prepreg obtained with air-coupled ultrasound system.

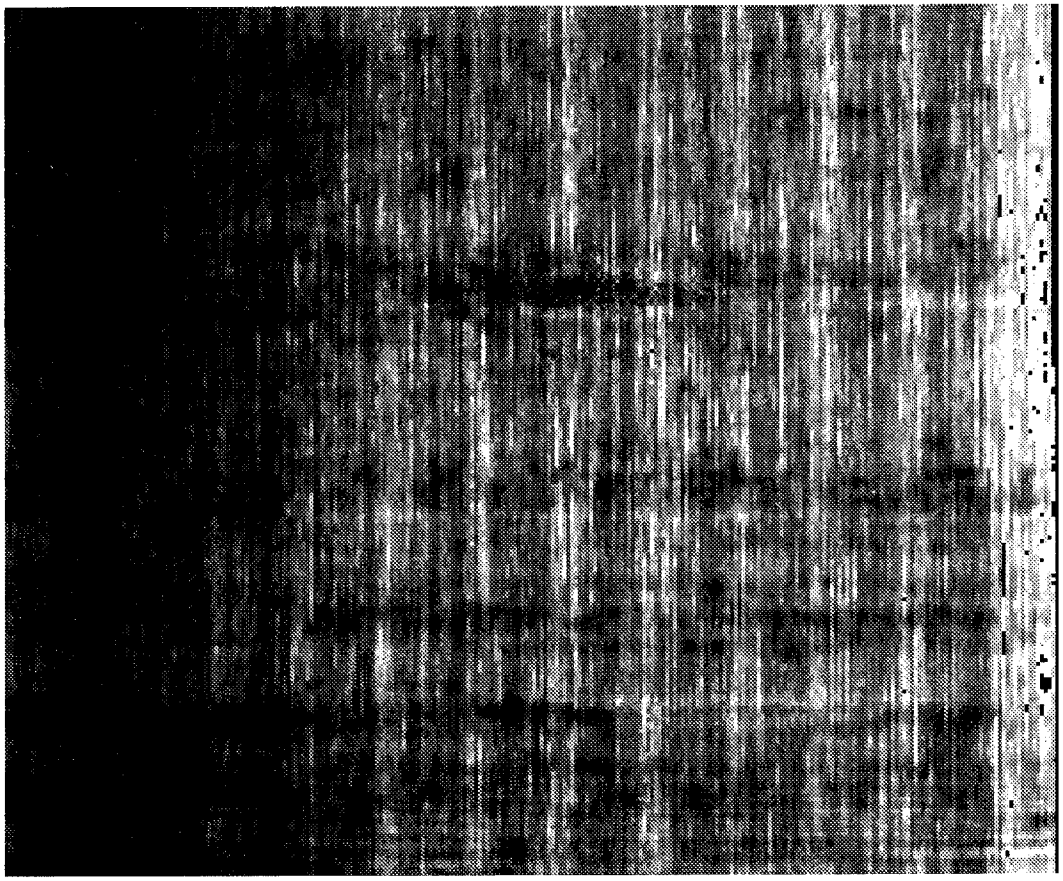

Figure 4. C-scan phase image of graphite-epoxy prepreg obtained with air coupled ultrasound system (same specimen as Fig. 3).

case, the ceramic is toughened by fibers which are only "mildly" adhered to the matrix. In fact, a large portion of the interfacial strength can be attributed solely to mechanical keying (frictional strength). Fibers toughen brittle ceramics by introducing additional stress (strain) relief and crack impeding mechanisms. The ceramic matrix composites are toughened primarily using fiber pull-out as a stress (strain) relief mechanism. Fracture energy is also consumed by crack propagation around fibers.

Since these strain relief mechanisms are essential, the quality of the fiber-matrix interface is of the utmost importance. In the case of ceramic-matrix composites, the optimal bond seems to be a "weak" one in comparison to most composite systems. The bond should be strong enough to allow a substantial amount of energy release during fiber pull-out. The consequence of too strong a bond is that it causes a propagating crack not to "see" the fiber and causes the material to behave as a monolithic brittle material. Ceramic-matrix composites depend upon fiber reinforcement primarily for toughening mechanisms, not modulus enhancement.

The polariscope constructed for measurement of residual stress in optically translucent ceramic matrix composites was distinctive because a laser was used as an intense monochromatic source while the optical data was stored digitally using a CCD camera and an image acquisition board in a computer, **Figure 5**. Since the HeNe laser used was a highly coherent source, a spinning ground glass disk rotating at 1800 rpm was added as a coherency scrambler to avoid interference fringes. The diverging beam from the disk was then recollimated through a 50mm focal length lens. After the laser beam passed through the polarizing optics and test composite it was imaged by a Nikon macro lens onto a Pulnix TM-745 CCD camera with a disabled automatic gain control. The data acquired from the camera was stored on a Data Translation frame grabbing board with 512 x 480 spatial resolution and an 8-bit gray scale.

Figure 6 is a schematic diagram and coordinate system for a single SiC tow in a 7740 glass matrix. **Figure 7** is the isochromatic image of residual thermomechanical stresses in the single tow specimen, while **Fig. 8** shows plots of the principal stresses for the single tow specimen along lines parallel to the y-axis at specified intervals of x.

For the cloth reinforced glass composite, a two-dimensional analysis was again performed. Since this specimen did not fulfill a plane strain condition as well as the single tow, a three-dimensional analysis would have been more accurate. This plane strain condition could be fulfilled by sub-slicing in order to achieve "thin" slices. However, sub-slicing is not a viable method for the direct

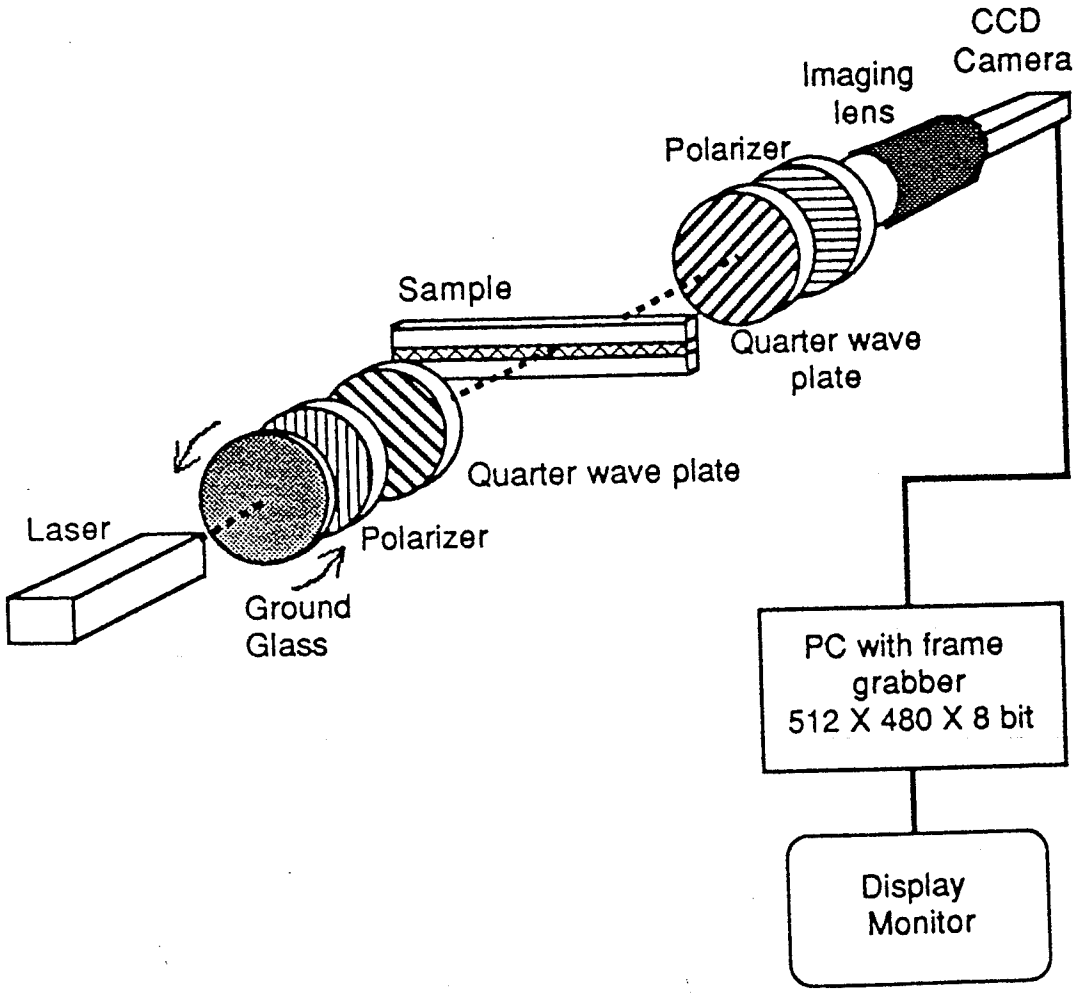

Figure 5. Schematic of polariscope and digital imaging system used for microphotoelasticity measurements.

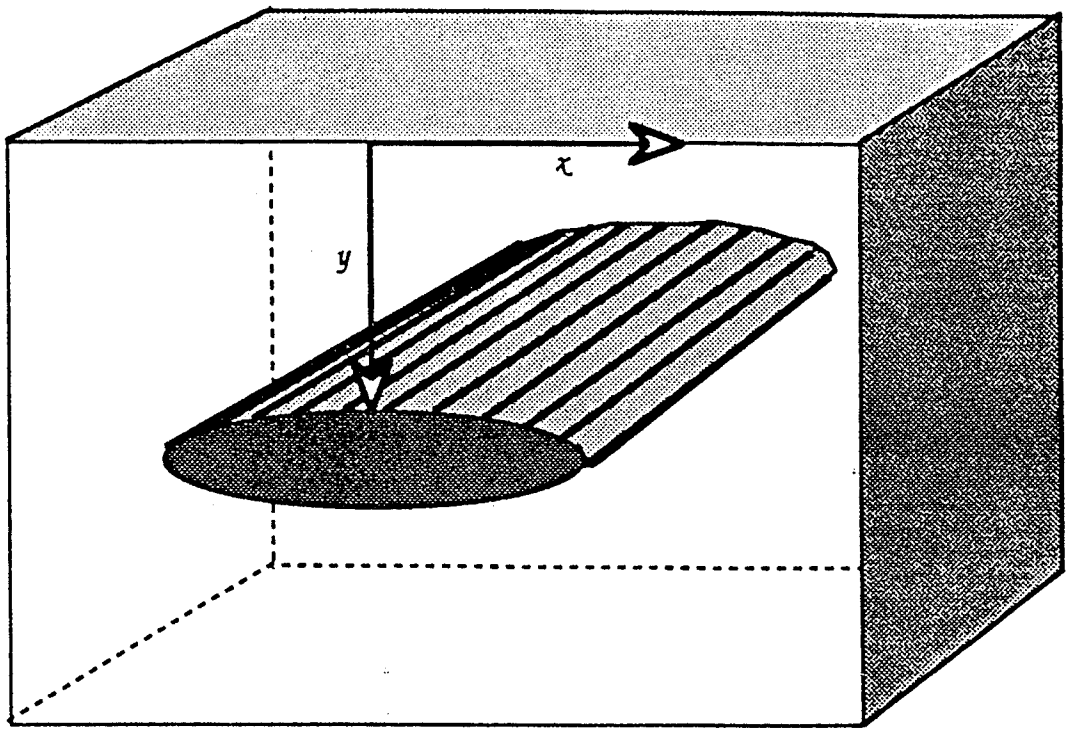

Figure 6. Schematic and coordinate system for single SiC tow in 7740 glass matrix.

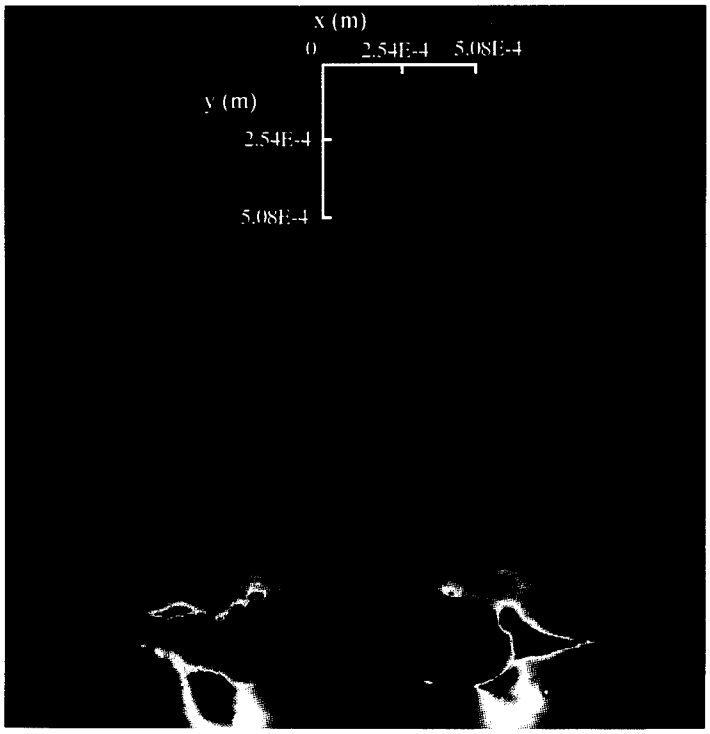

Figure 7. Isochromatic image of residual thermomechanical stress in single tow SiC/7740 glass ceramic matrix composite.

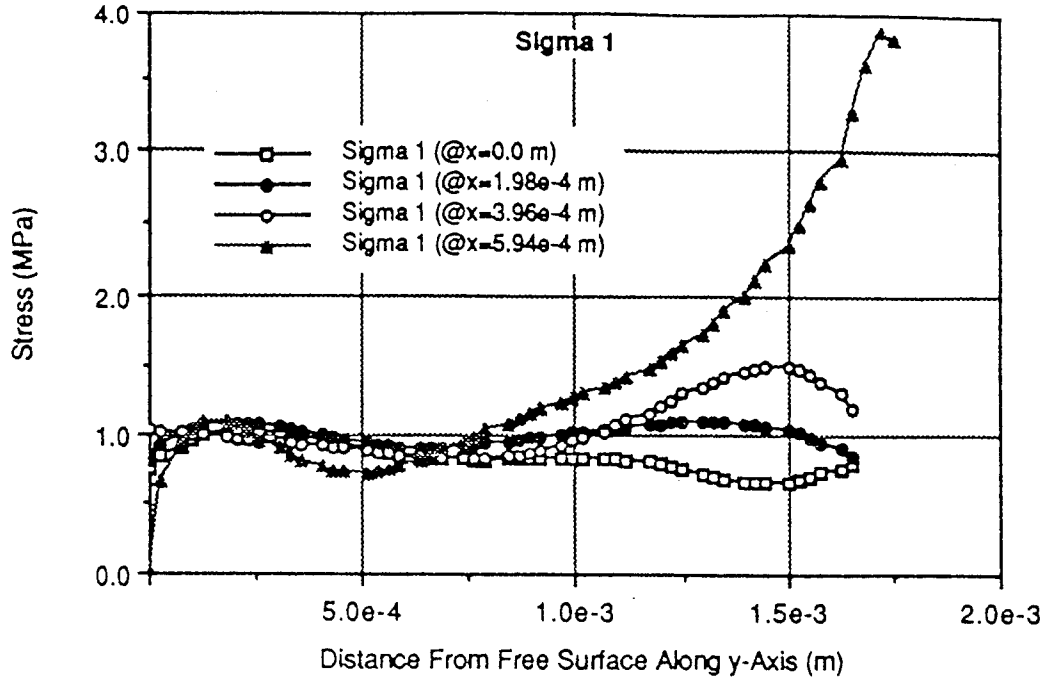

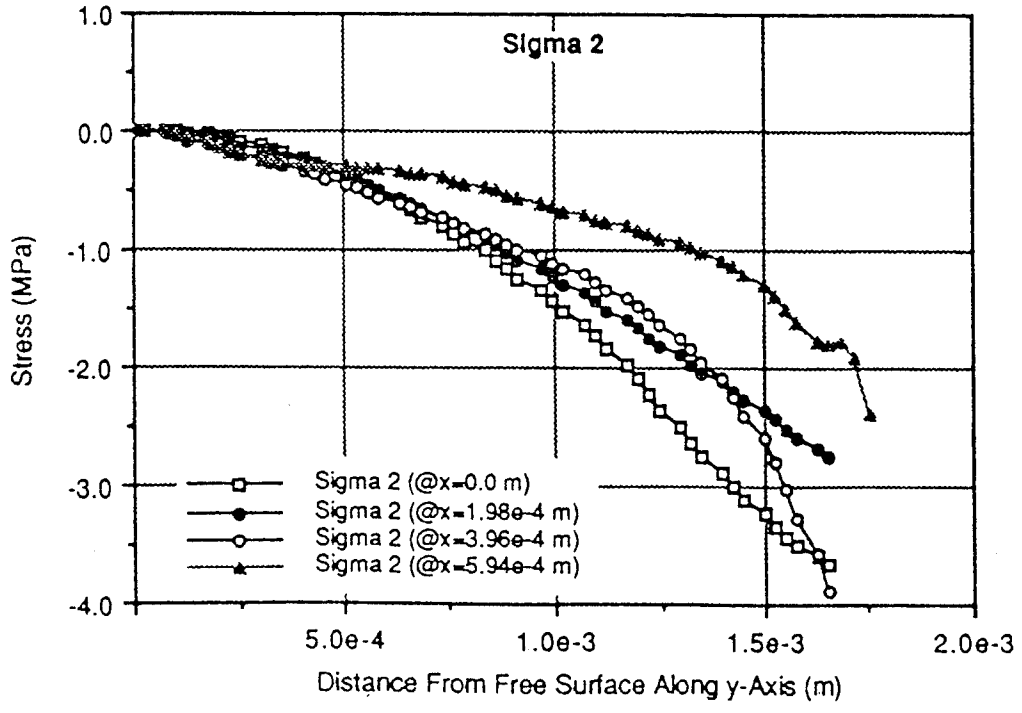

Figure 8. Plots of principal stresses for the single tow specimen along lines parallel to the y-axis at specified intervals of x.

observation of stresses in the present composite system. None-the-less, the two-dimensional analysis is valuable in understanding processing stresses since it does provide a local stress profile. However, the profile is lower than actual although the line along which the stresses were measured was performed at a location in which the three dimensional effects were minimal. A schematic and the coordinate system selected for this specimen are shown in **Fig. 9** and the isochromatic image of residual thermomechanical stresses are shown in **Fig. 10**.

In order to separate the stresses, integration lines were taken close to the line at $z = 0$. These lines possessed relatively small three-dimensional effects. Based on the two-dimensional analysis, the stresses were separated along the y-axis at $x = z = 0$. **Figure 11** shows a plot of the separated principal stresses for the cloth reinforced ceramic matrix composite.

Detection of Composite Defects
(Fiber breaks, Cracks, Voids, Delaminations)

As a precurser to the present research a number of nondestructive evaluation methods were investigated for detection of defects in composites. These included ultrasonic A-, B-, and C-scans and ultrasonic attenuation, ultrasonic second harmonic generation, and acoustic emission for continuous monitoring of damage development during mechanical tests. Several laser ultrasonic systems were adapted to serve as non-contact generators and/or detectors of ultrasonic waves in the composite materials. Although these systems have been used for conventional pulse-echo, through transmission ultrasonics, acousto-ultrasonics, and acoustic emission testing on metals, the poor optical reflectivity of most of the composites investigated prevented optimum use of these techniques. Laser speckle decorrelation proved to be extremely sensitive to very early fatigue damage development in some specimens. Pulsed heating thermography, vibrothermography, and radio-opaque penetrant assisted x-radiography systems were also used for damage assessment. Although the techniques of nuclear magnetic resonance imaging and electron paramagnetic resonance imaging are able to determine the state of degradation of a number of polymeric materials, experiments run on the magnetic resonance imaging research facility at The Johns Hopkins University Medical Institution showed that conventional medical systems cannot be used successfully on graphite/epoxy or metal matrix composites because of the high electrical conductivity.

Therefore, the most practical overall method chosen for the present research was ultrasonics. A survey ultrasonic c-scan system was used initially followed in detected problem areas by a more detailed and precise acoustic

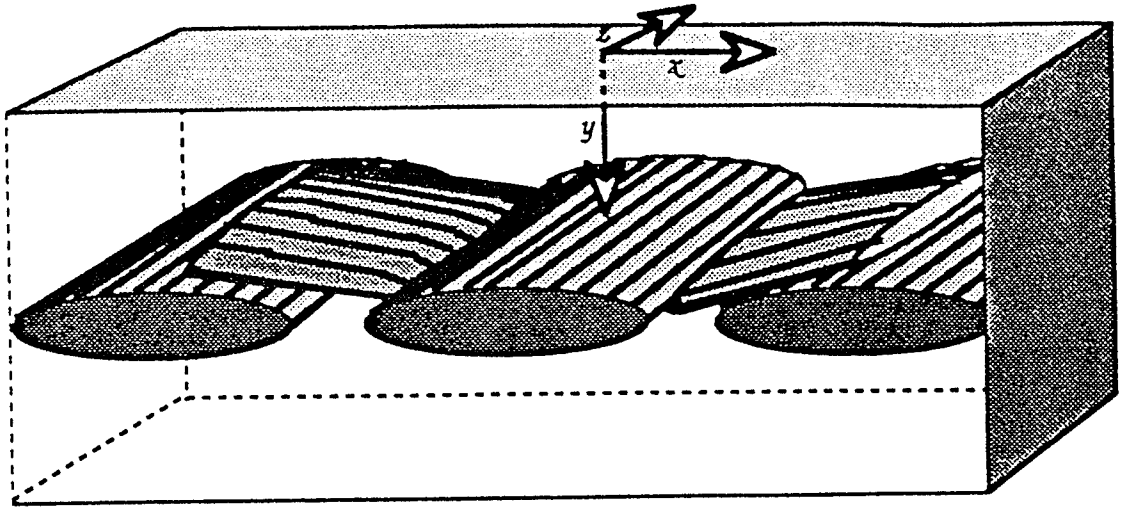

Figure 9. Schematic and coordinate system for two-dimensional SiC cloth reinforced 7740 glass ceramic matrix composite.

Figure 10. Isochromatic image of residual thermomechanical stress in two-dimensional SiC cloth reinforced 7740 glass ceramic matrix composite.

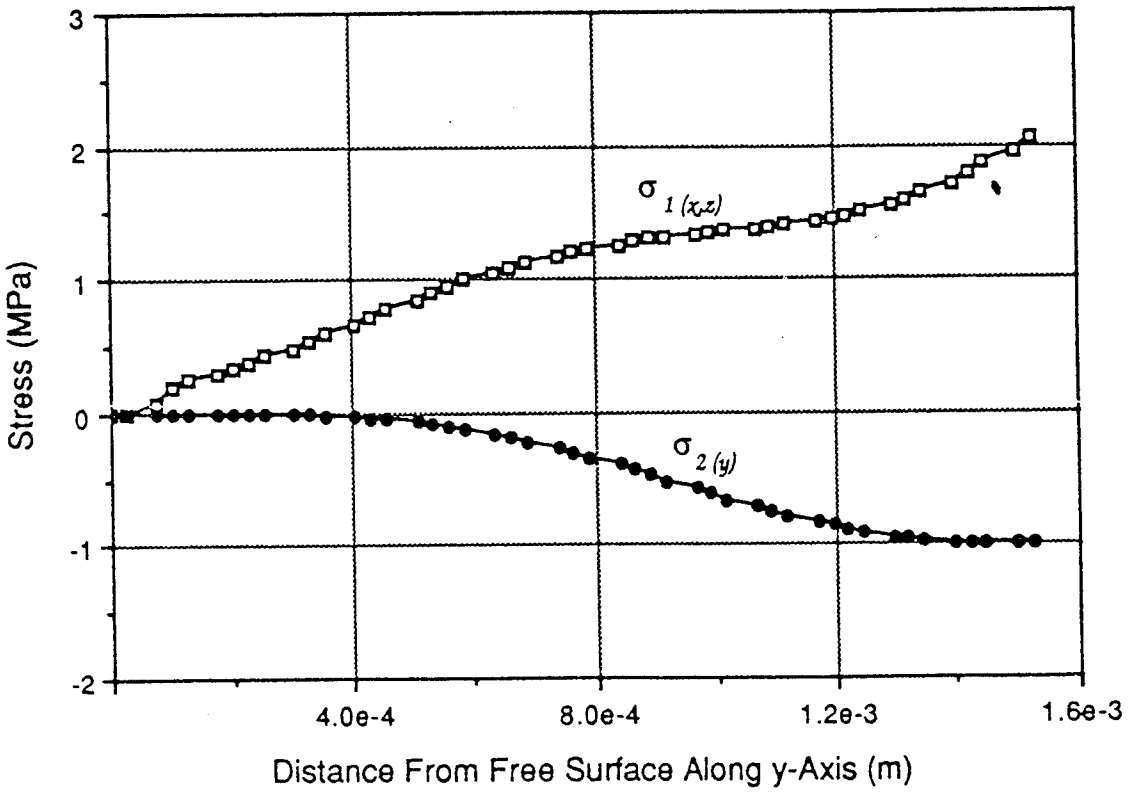

Figure 11. Plots of principal stresses for the two-dimensional SiC cloth reinforced specimen along y-axis at x = 0, and y = 0.

(ultrasonic) microscope examination. The ultrasonic system used for this work was a high resolution acoustic microscope (Micro-Scan IC by Sonix Inc.) which consists of a fully digitized integrated inspection package. Data acquisition is performed with a 100 MHz waveform digitizer and equivalent time sampling rates of up to 3.2 GHz. A 64K high speed static RAM allows for extremely high data throughput which means thousands of waveforms can be saved per second during inspection. A digitally controlled -600 VDC spike pulser with repetition rate of from 1 Hz to 10 kHz controls the electrical excitation of the sending portion of the system. The receiver also is digitally controlled and has a bandwidth of 1-200 MHz with gain of up to 50 dB and an attenuator of from 0 to -60 dB which is digitally selectable in 1 dB increments. The scanning bridge for this system utilizes an optical quality translation table with raster step increments as small as 10 microns capable of accuracy and repeatability in the 1-2 micron range. Among the defects, delaminations were easiest to find, followed by voids, cracking, and porosity. Porosity tended to be difficult to reliably detect with conventional ultrasonic testing, but attenuation and second harmonic generation methods showed some promise. Delaminations were found routinely in thin laminates. In thick-section composites breakage of fiber tows or serious ply gaps contributed to reduced mechanical properties, since lack of fiber continuity implies low stiffness for tensile or compressive loads applied across the flawed regions.

A series of typical acoustic (ultrasonic) microscope C-scan images of several different composite specimens are shown in **Figures 12-17**. **Figure 12** is a scan of a graphite-epoxy prepreg showing misplaced fibers on the ply surface as well as variation in resin content over the entire area of the prepreg. **Figure 13** shows amplitude plots from an acoustic microscope scan of a quasi-isotropic fiber reinforced graphite-peek laminate. By application of time gates on the returning pulse inhomogenieties on the individual plies were imaged. **Figure 14** is an amplitude plot of a woven fiber reinforced polymer plate. As seen the manufacture of this plate is fairly uniform and of relatively high quality. **Figure 15** is an amplitude plot of a carbon-carbon composite plate showing a large number of inhomogenieties both in size and spatial distribution. **Figures 16 and 17** are amplitude plots of a metal matrix (graphite fibers in aluminum matrix) composite plates showing inhomogenieties and fiber wrinkles (particularly evident in higher frequency 25 MHz scan). The dark areas at the top of both figures are due to gas entrapped in the composite during manufacture.

Figures 18-22 show optical photographs of defects commonly found in composite materials. **Figure 18** shows an

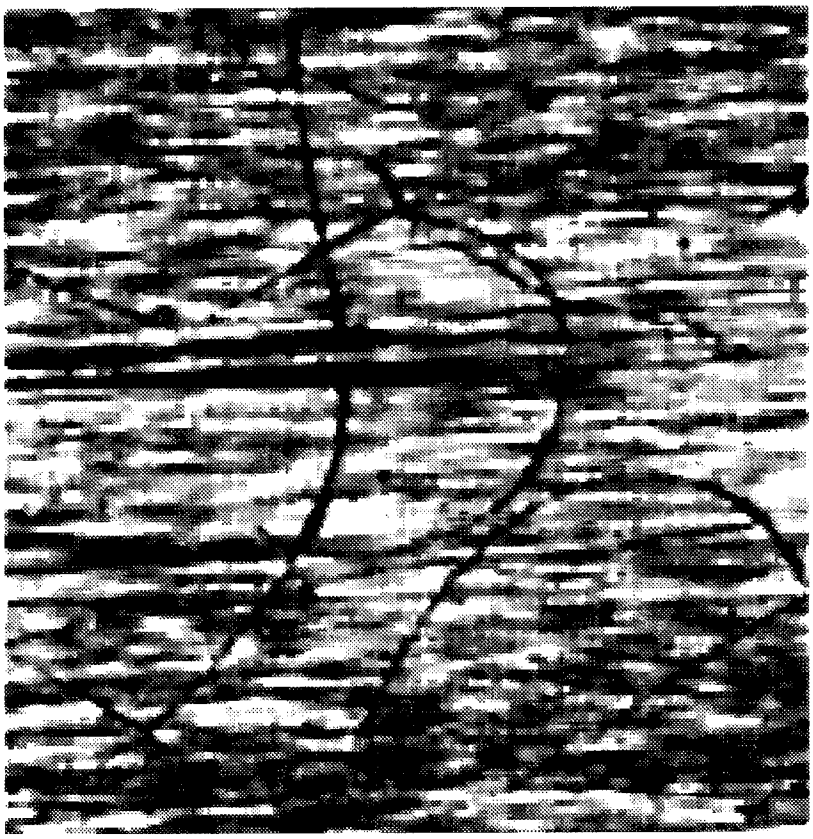

Figure 12. Acoustic microscope scan of graphite-epoxy prepreg showing misplaced fibers on ply surface. 100 MHz spherically focused transducer. Scan area 0.4" x 0.4".

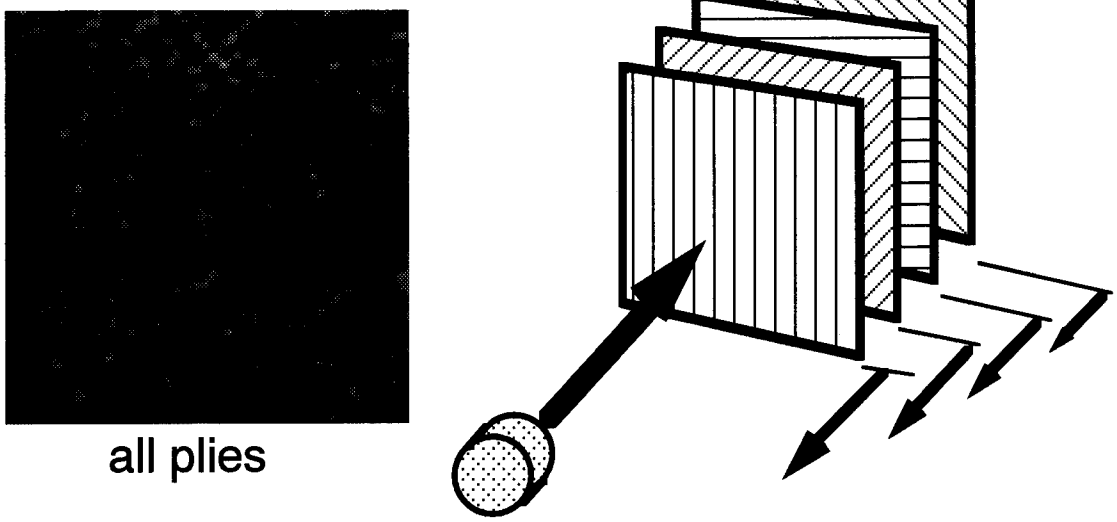

all plies

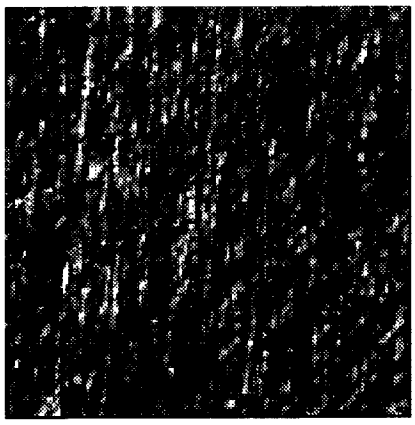

0

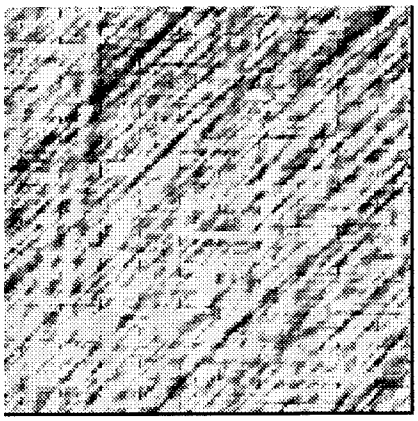

+45

90

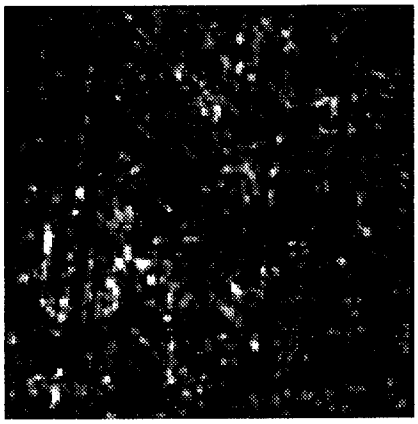

-45

Figure 13. Amplitude plots from acoustic microscope scan of quasi-isotropic fiber reinforced polymer laminate. Pulse-echo mode using 75 MHz spherically focused piezoelectric transducer. Scan area 0.2"x 0.2".

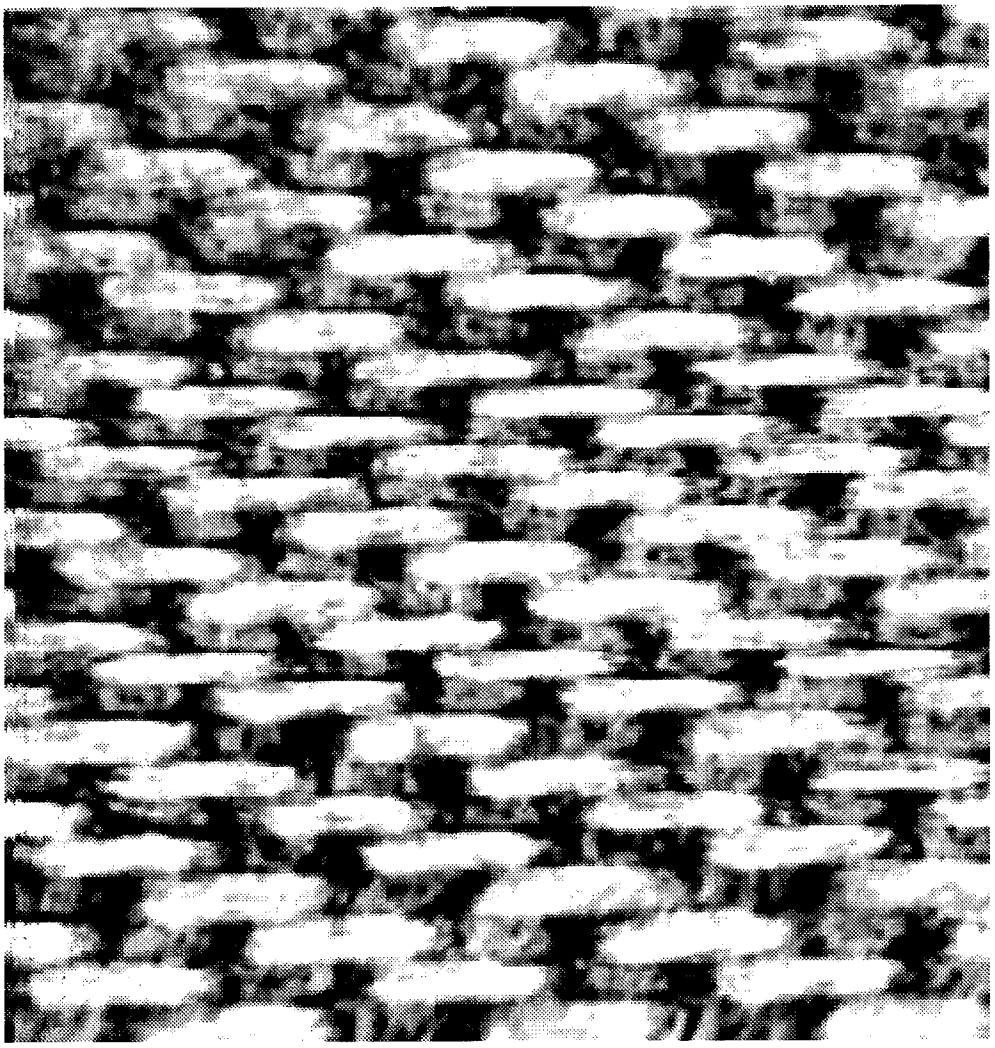

Figure 14. Amplitude plot from acoustic microscope scan of woven fiber reinforced polymer plate. Pulse-echo mode using 25 MHz spherically focused piezoelectric transducer. Scan area 0.75"x 0.75".

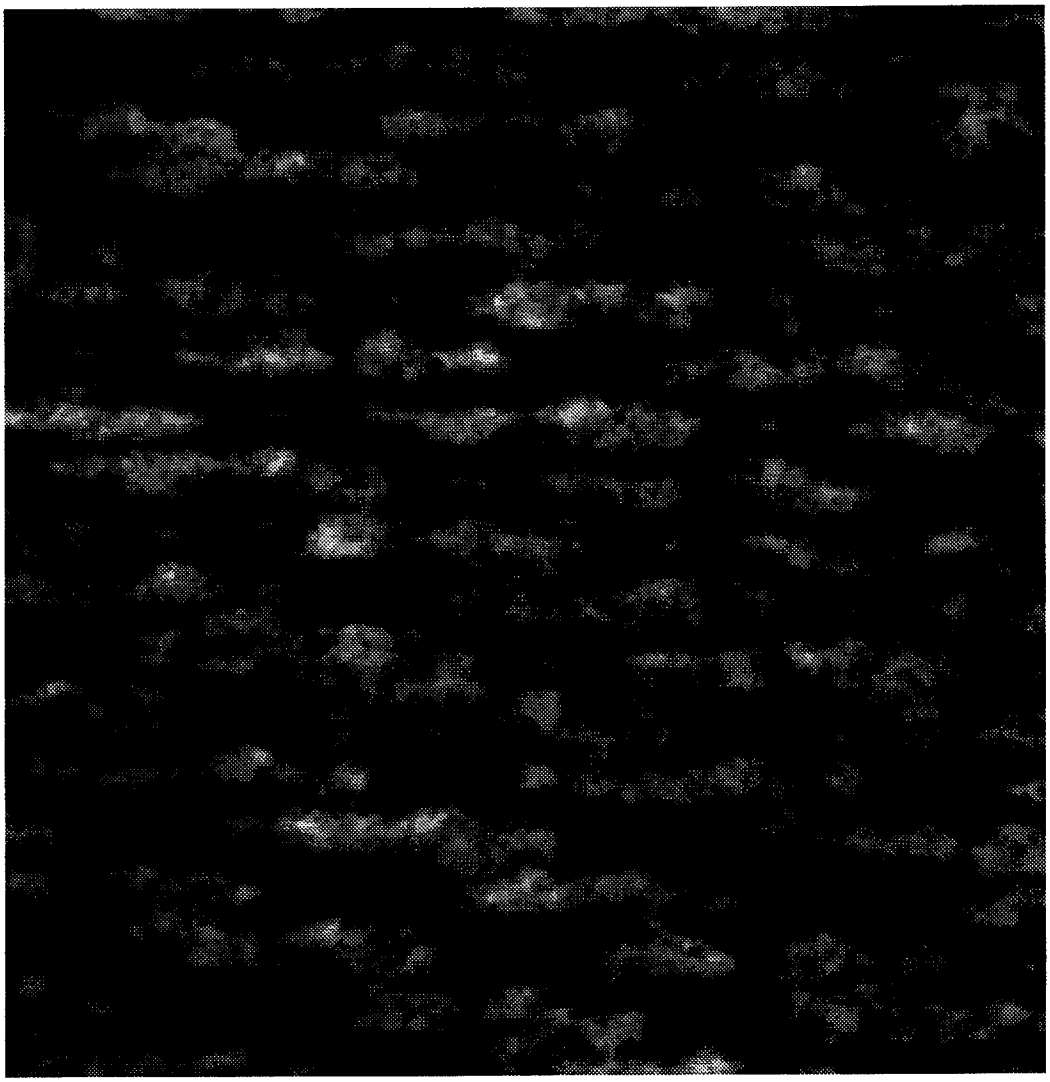

Figure 15. Amplitude plot from acoustic microscope scan of carbon-carbon composite plate. Pulse-echo mode using 25 MHz spherically focused piezoelectric transducer. Scan area 0.75"x 0.75".

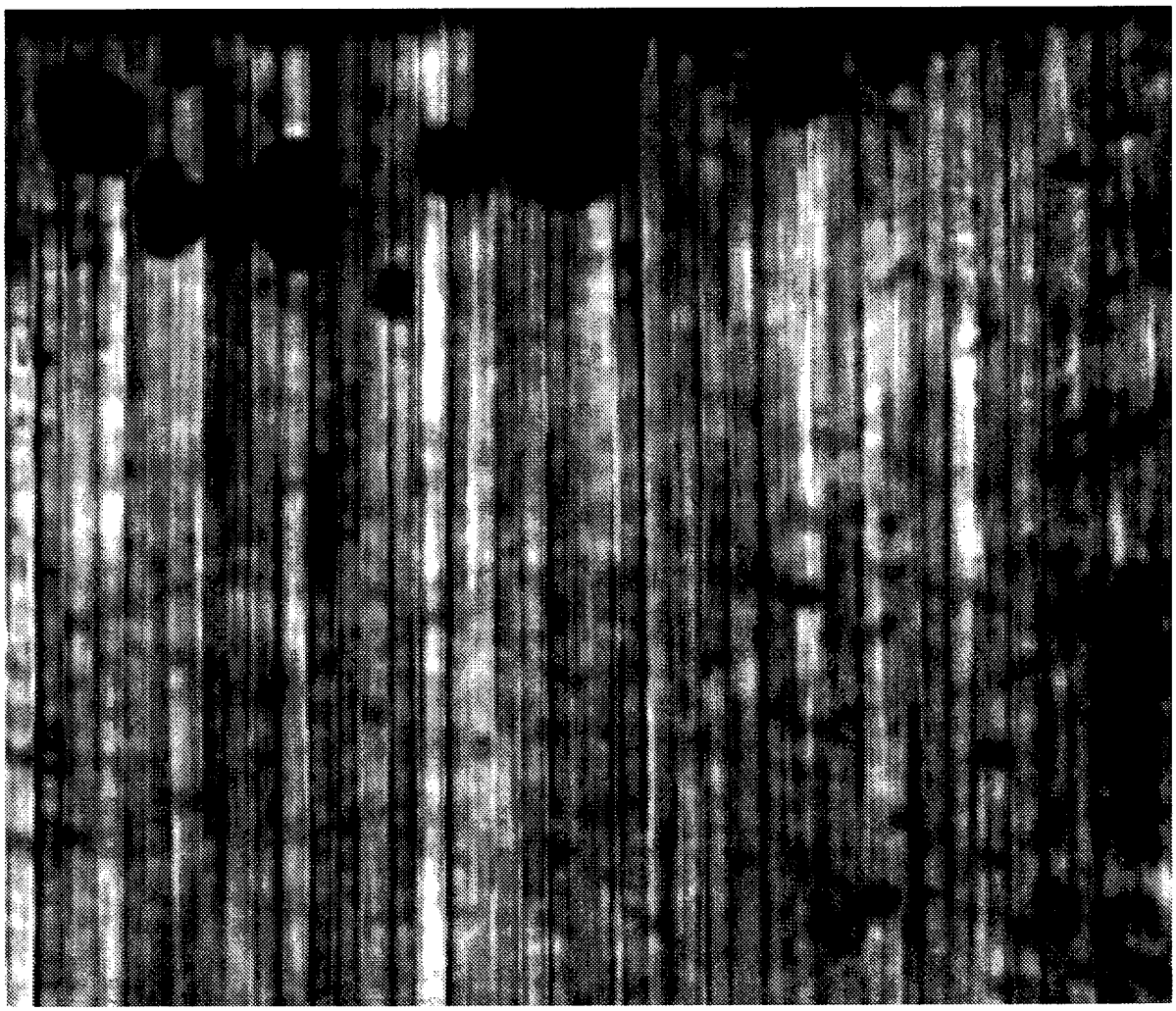

Figure 16. Amplitude plot from acoustic microscope scan of metal matrix composite plate. Through transmission mode using 15 MHz spherically focused piezoelectric transducers. Scan area 1"x1".

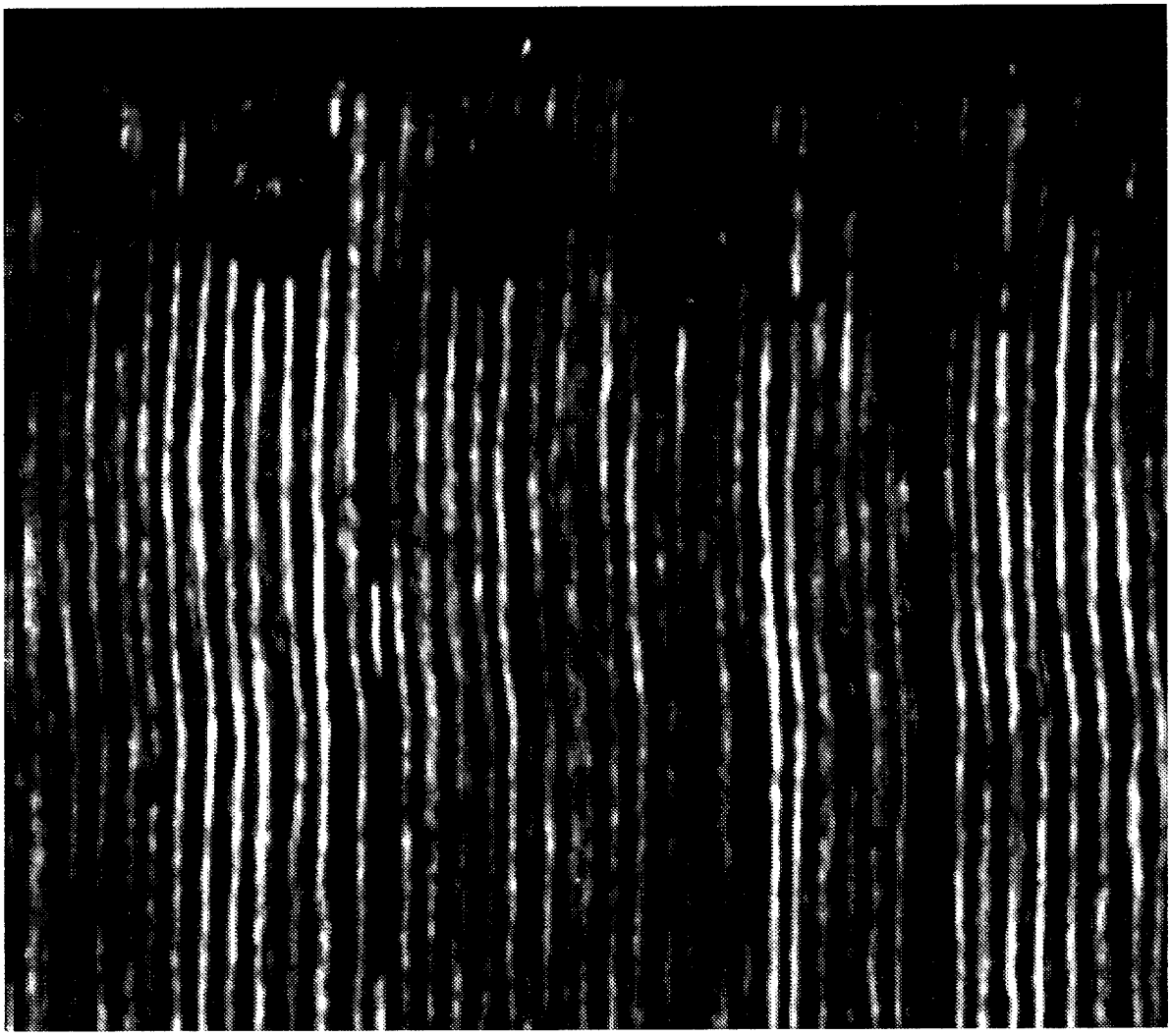

Figure 17. Amplitude plot from acoustic microscope scan of metal matrix composite plate. Pulse-echo mode using 25 MHz spherically focused piezoelectric transducer. Scan area 1"x1".

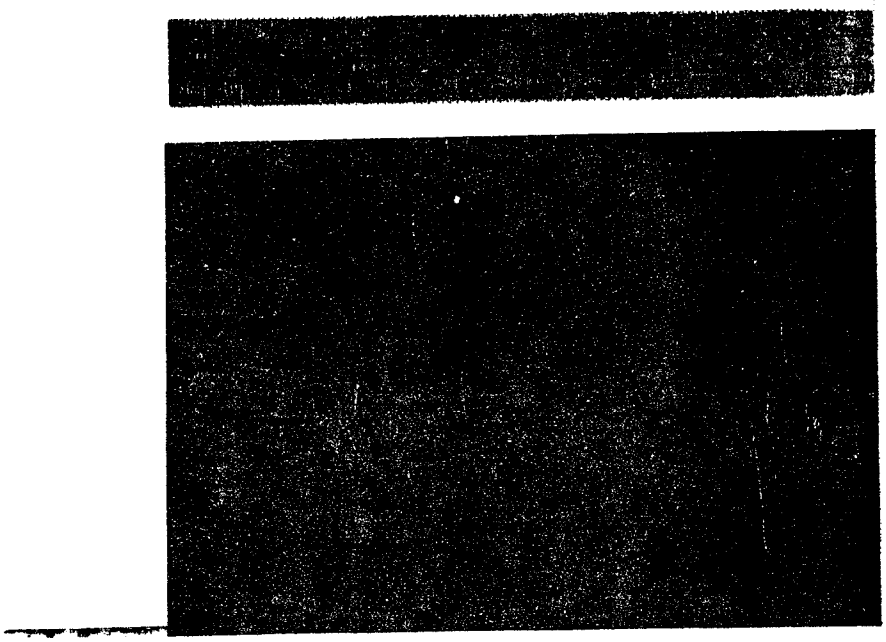

Figure 18. Photograph of uncured graphite-epoxy prepreg showing misplaced fibers on lamina surface. Also shown is debris on surface picked up during handling. Fiber direction is parallel to the ruler.

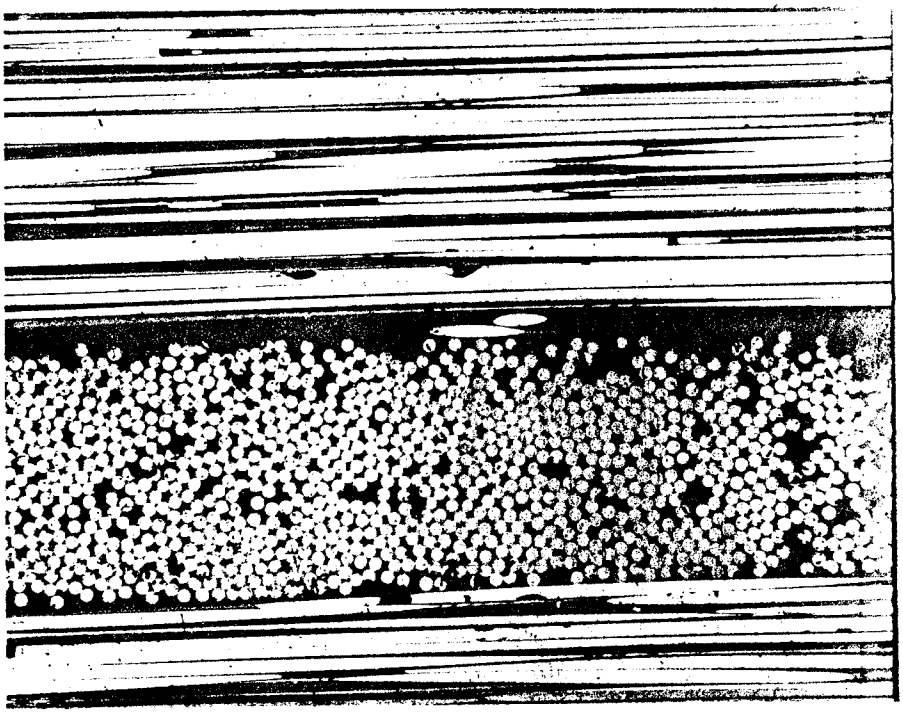

Figure 19. Photomicrograph of graphite-epoxy laminate showing effect of misplaced fiber. Result is a resin rich region at lamina interface.

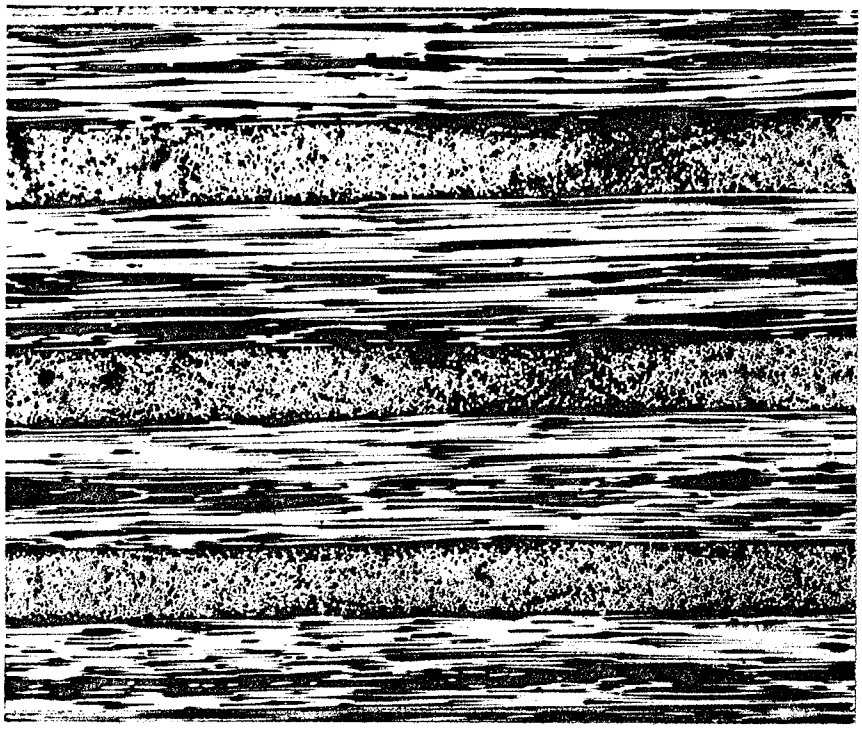

Figure 20. Photomicrograph of graphite-epoxy laminate showing regions of resin rich laminae. These defects can be a result of the manufacture of the prepreg or can occur during laminate cure.

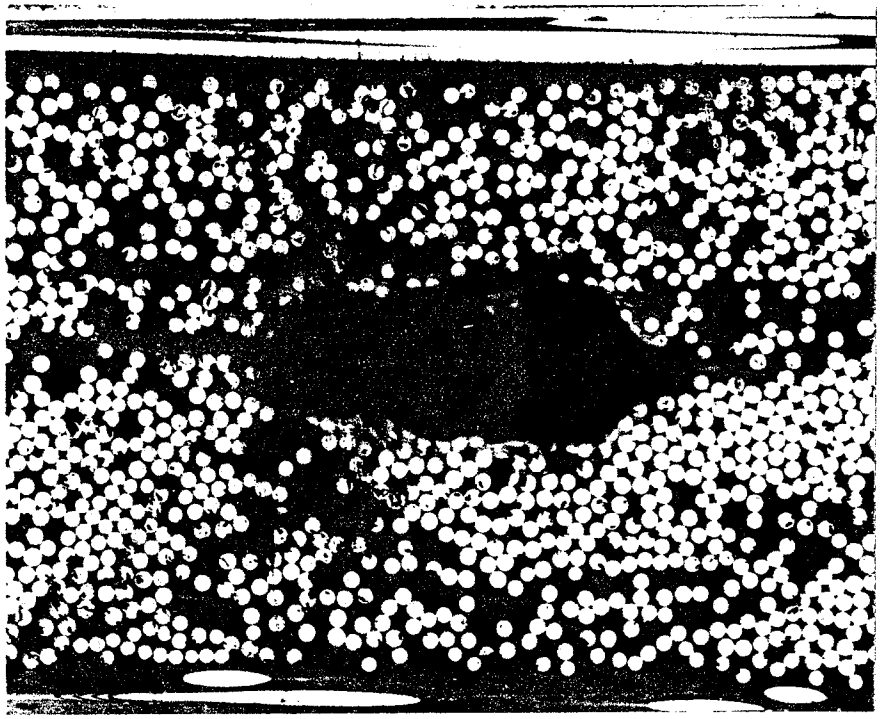

Figure 21. Photomicrograph of graphite-epoxy laminate showing void commonly produced during autoclave cure.

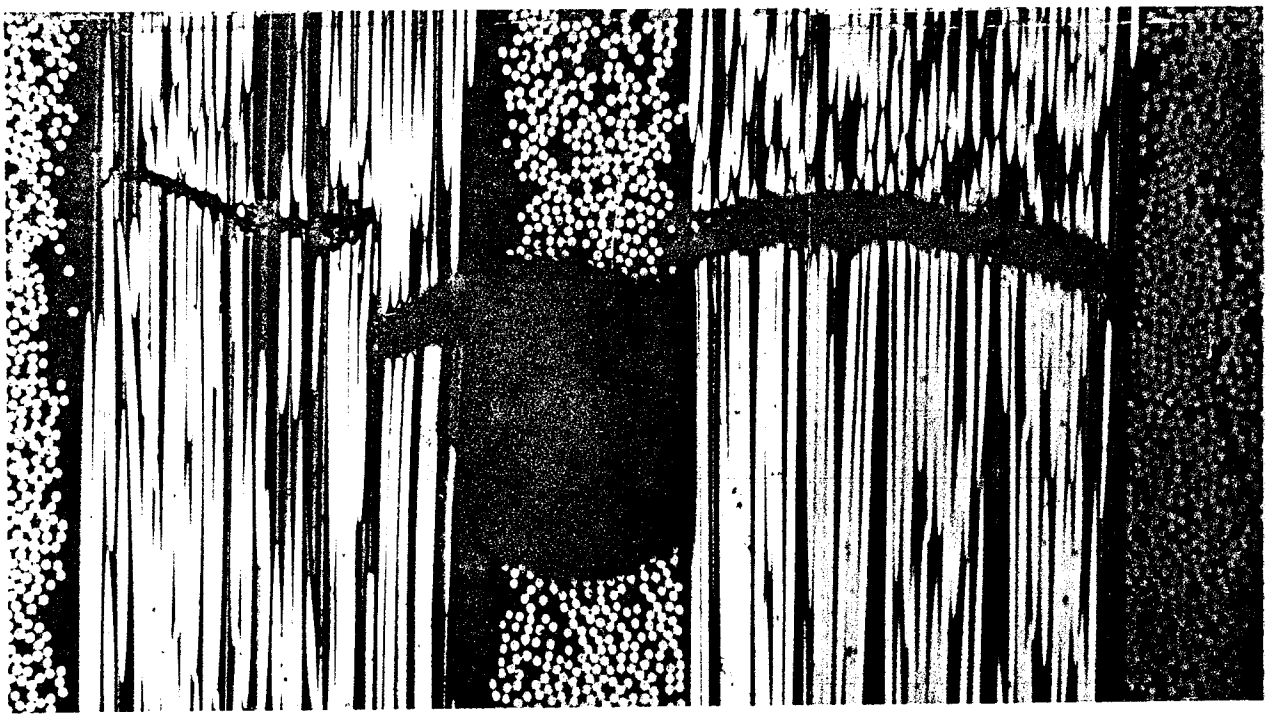

Figure 22. Photomicrograph of graphite-epoxy laminate showing processing void with interlaminar crack passing through it.

uncured graphite-epoxy prepreg with misplaced fibers on the surface of the lamina. Also shown is debris on the surface picked up during handling. Fiber direction is parallel to the ruler. **Figure 19** shows a graphite-epoxy laminate with a misplaced fiber which causes a resin rich region at the lamina interface. **Figure 20** shows a graphite-epoxy laminate with regions of resin rich laminae. These defects can be a result of the manufacture of the prepreg or can occur during laminate cure. **Figure 21** shows a void in a graphite-epoxy laminate produced during autoclave cure. **Figure 22** shows a graphite-epoxy laminate containing a processing void with an interlaminar crack passing through.

Detection of Fatigue Induced Defects

Since military aircraft experience severe vibrations, and since, there is a current problem with fatigue damage in aircraft constructed from metal, consideration was given to nondestructive detection of fatigue damage in composites.

Fatigue damage in composites is much more complicated than in monolithic metals, ceramics, or polymers. That is because there are so many more sources of defects in composites compared with monolithic solids. Fatigue damage in composites is characterized by initiation and growth of cracks from multiple sites throughout the entire volume of the material. Nevertheless, composites perform very well under cyclic loading. Their inherent inhomogeneity and anisotropy, despite presenting multiple locations for a variety of damage modes to occur, serves to enhance their ability to withstand fatigue. Fibers act as crack arrestors, while lamina serve as both crack arrestors and deflectors.

Since most fatigue tests on composite materials have been performed in tension-tension or tension-compression on relatively long, thin laminates, it has been possible to give a rough scenario of fatigue damage development in these cases. Stage one consists of matrix cracks and fiber breaks. Stage two consists of crack coupling, interfacial debonding, delaminations, and fiber breaks. Stage three consists of delamination growth, increased fiber breaking, and finally fracture.

Most of the compression tests on composite materials have suffered from the fact that the test specimen configuration was similar to those normally used in tensile tests, that is long thin specimens. The use of such specimens often does not yield correct compression response data, because of long column buckling problems. In some cases the test specimens were restrained from buckling by side supports which makes the resulting data even more questionable.

Recently, compression-compression fatigue tests have been run on relatively thick composite specimens 3" in length, possessing 1" square cross-sections. This 3 to 1 aspect ratio corresponds to that recommended for metal compression test specimens by ASTM. The material used was Hercules AS4/3501-6 graphite-epoxy prepreg. The prepreg was stacked into panels measuring twelve inches square with one inch nominal thickness and autoclave cured. Each panel was cut into a number of compression test specimens with stress concentration notches of 1/8" radius in the through thickness direction at the mid height of each side. These were implemented to localize stress induced damage so that nondestructive evaluation techniques could be optimally applied. **Figure 23** is a schematic drawing of the compression-compression fatigue test specimen.

A large number of compression-compression fatigue and quasi-static uniaxial compression tests were performed on over 50 specimens while being monitored by various NDE techniques. Results indicate a minimum of 20% reduction in specimen strength due to the stress concentration notches. Unnotched specimens did not fail when loaded to the capacity of the mechanical load frame. Thus, material strength was found to exceed 125 ksi. Stiffness reduction, mechanical hysteresis, and permanent deformation during fatigue were observed. Mechanical hysteresis was determined to result from the presence of the stress concentration notches. Changes in mechanical characteristics have been observed after the first cycle of a fatigue test.

Damage mechanism characterization has been performed on a large number of fatigue damaged specimens. Ultrasonic B- and C-scans have been used to locate and identify delaminations, interlaminar cracks, and intralaminar cracks. Penetrant enhanced x-ray radiography has identified delaminations, interlaminar cracks, and longitudinal and transverse matrix cracks. Optical microscopy on cut and polished sections of fatigue damaged composites identified delaminations, interlaminar cracks, kink bands, and longitudinal and transverse matrix cracks. The results from these techniques has verified that damage occurs with the first cycle of a fatigue test.

Figure 24 is an acoustic (ultrasonic) microscope amplitude scan of a compression-compression fatigue damaged graphite-epoxy cross ply laminate with ultrasonic beam perpendicular to the laminae. **Figure 25** is an acoustic (ultrasonic) microscope amplitude scan of a compression-compression fatigue damaged graphite-epoxy cross ply laminate with ultrasonic beam parallel to laminae. Same specimen as shown in **Fig. 24**. **Figure 26** is a time of flight scan of the same specimen with the same orientation as in **Fig. 25**. **Figure 27** is a photomicrograph of a transverse matrix crack in a graphite-epoxy cross ply laminate which

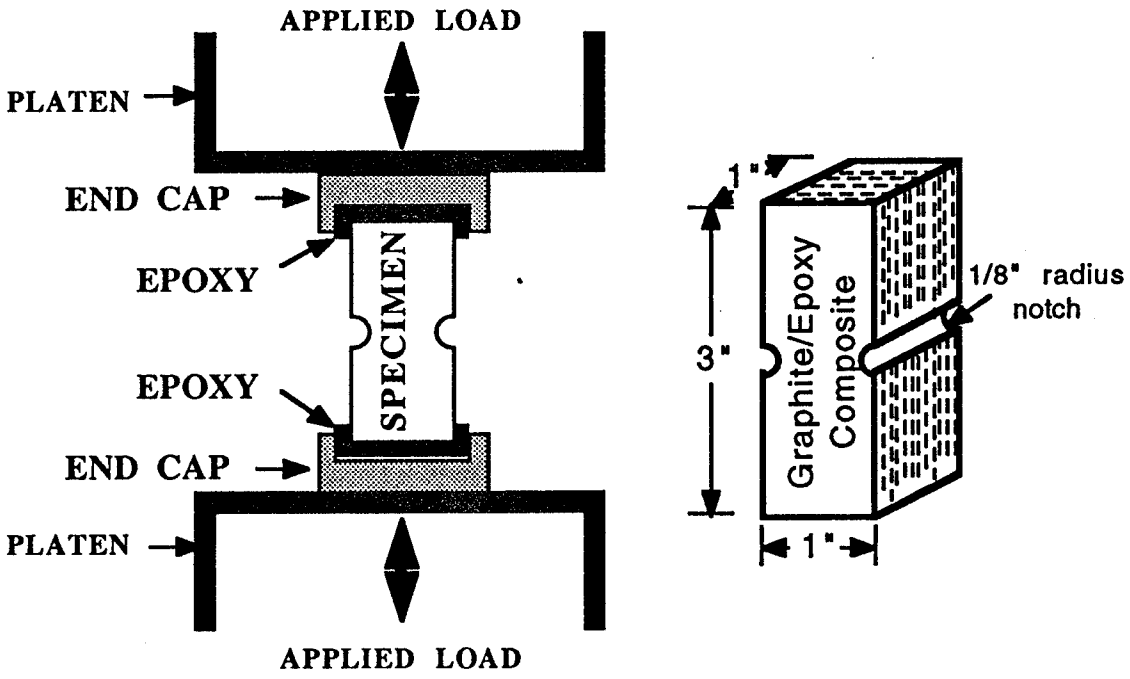

Figure 23. Schematic drawings of compression-compression fatigue fixture and graphite-epoxy fatigue test specimen.

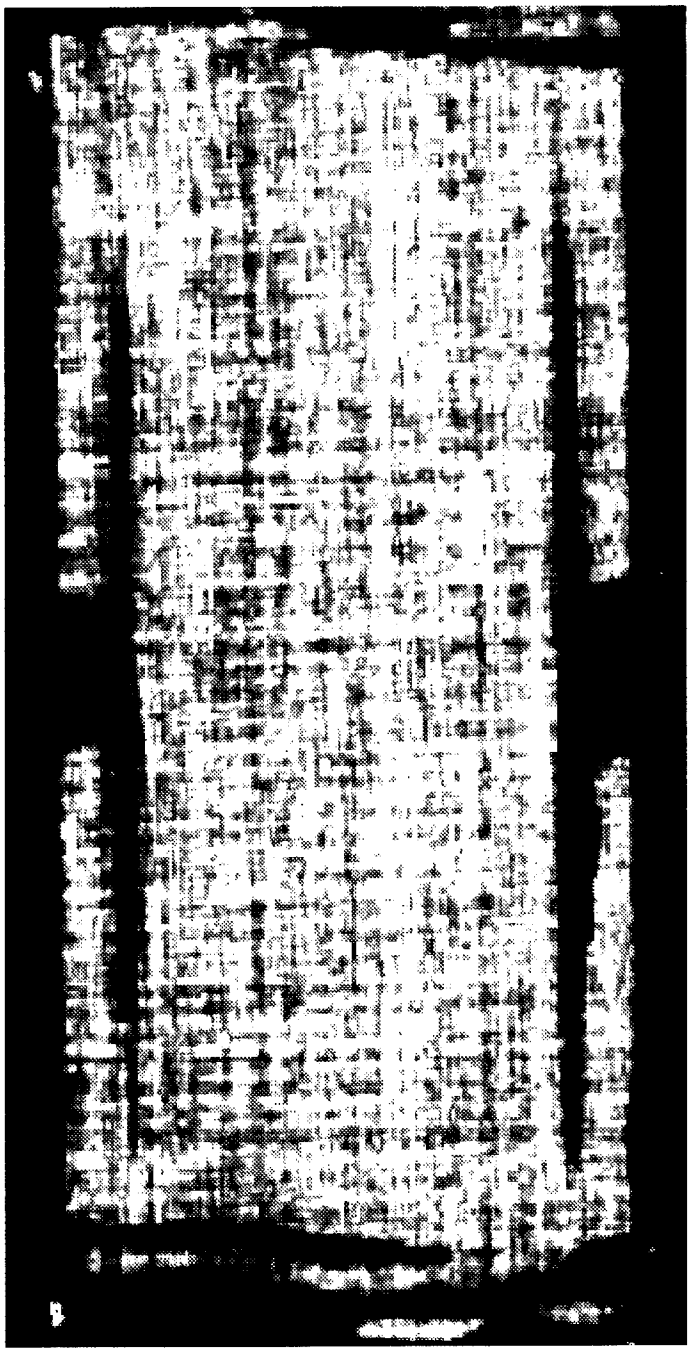

Figure 24. Amplitude plot from acoustic microscope scan of compression-compression fatigue damaged graphite-epoxy cross ply laminate with ultrasonic beam perpendicular to the laminae. Pulse-echo mode using 25 MHz spherically focused transducer. Scan area 1.25" x 2.5".

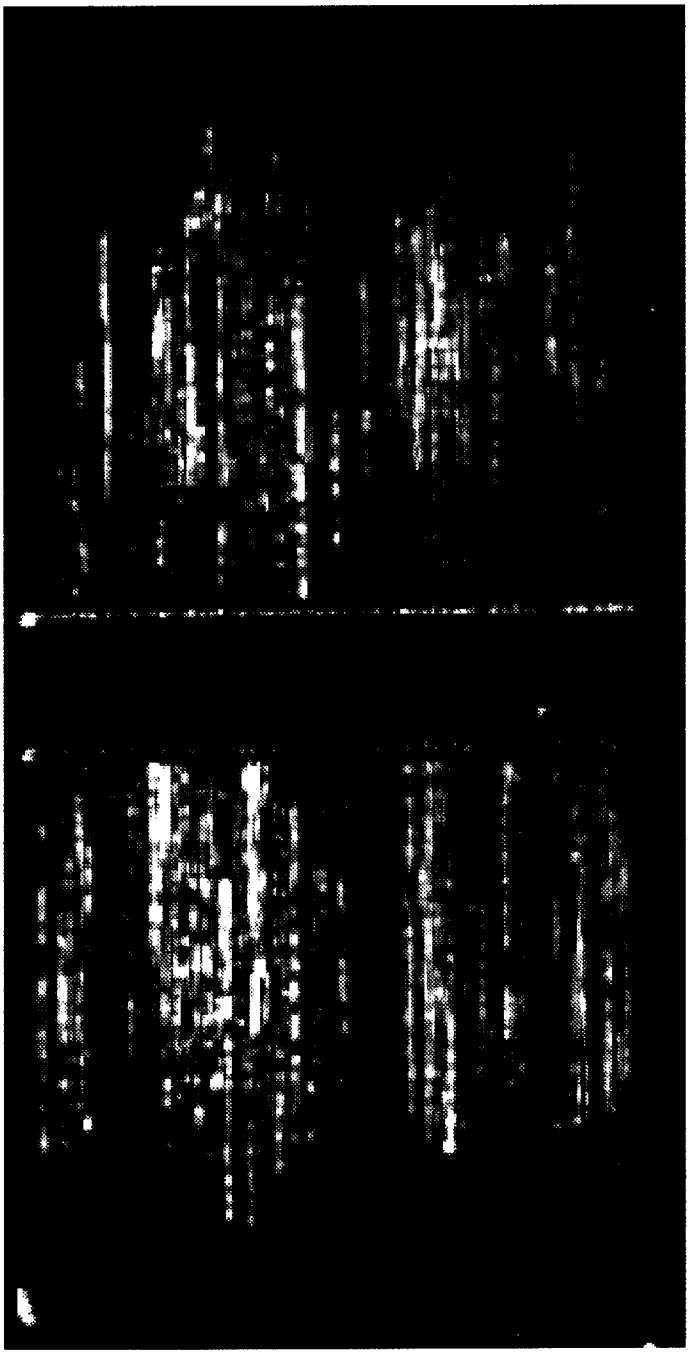

Figure 25. Amplitude plot from acoustic microscope scan of compression-compression fatigue damaged graphite-epoxy cross ply laminate with ultrasonic beam parallel to laminae. Pulse-echo mode using 25 MHz spherically focused transducer. Same sample as in Fig. 24.

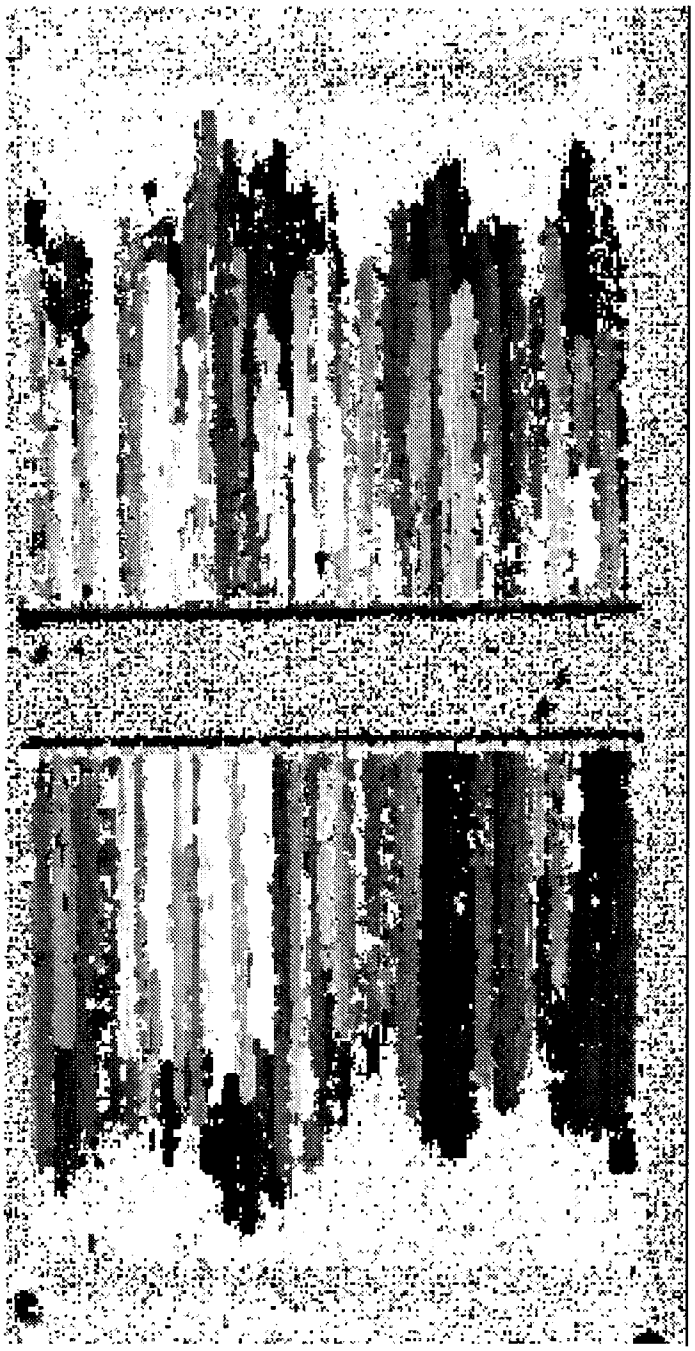

Figure 26. Time of flight plot from acoustic microscope scan of compression-compression fatigue damaged graphite-epoxy cross ply laminate with ultrasonic beam parallel to laminae. Pulse-echo mode using 25 MHz spherically focused transducer. Same sample and view as in Fig. 25.

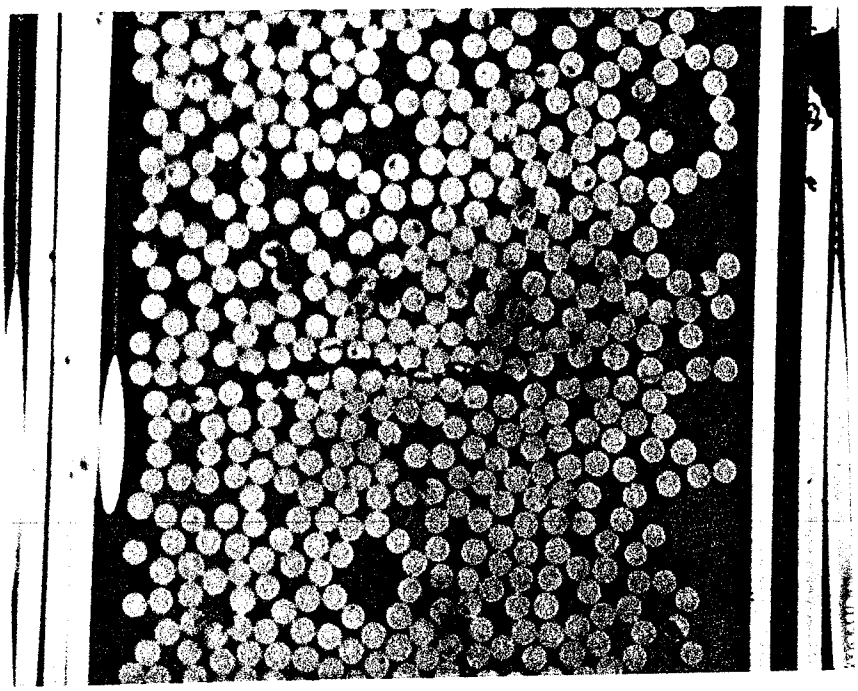

Figure 27. Photomicrograph of transverse matrix crack in graphite-epoxy cross ply laminate which was induced by compression-compression fatigue.

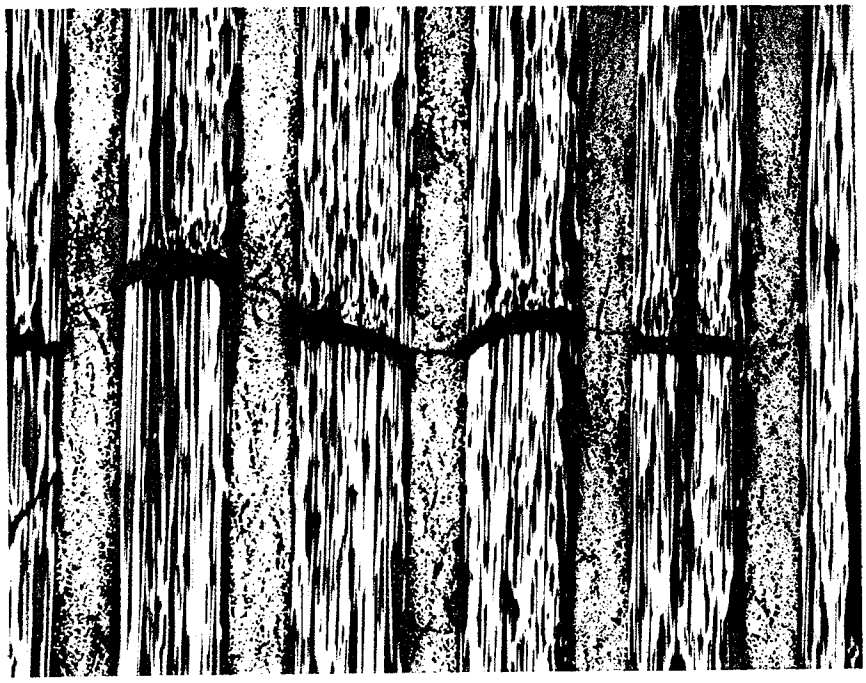

Figure 28. Photomicrograph of interlaminar crack in graphite-epoxy cross ply laminate which was induced by compression-compression fatigue.

was induced by compression-compression fatigue. **Figure 28** is a photomicrograph of an interlaminar crack in a graphite-epoxy cross ply laminate which was induced by compression-compression fatigue.

Specimen damage accumulation from compressive fatigue was characterized. It was found that both damage state and mechanical response of double edge notched specimens go through three stages as a result of uniaxial compression-compression fatigue loading and that correlations can be drawn between damage state and mechanical characteristics. It was found that during the fatigue test specimen stiffness and permanent deformation changed rapidly during the first few load cycles. That same state in fatigue life coincided with rapid production of matrix cracks. A second stage occurred in which there was gradual growth of matrix cracks and little change in mechanical characteristics. A third stage then occurred in which a critical crack propagated within the material causing failure. A dramatic change in mechanical characteristics often occurred in this third stage. It was found that composite compressive fatigue characteristics have some similarities to those reported in the literature on tensile fatigue. The greatest dissimilarity was that failure did not result from dispersed damage coalescing to destroy the load carrying capacity of the structure. Failure resulted from a single dominant flaw originating on the surface of the notch.

Contact ultrasonic methods were also used to evaluate fatigue damage in the thick double edge notched specimens. Pulse-echo and through-transmission techniques were used with transducers having nominal frequencies of 0.5, 1.0, and 2.0 MHz. The transducers were excited with either a spike pulse or a high power tone burst waveform. The received signal was digitized with a 100 MHz digital oscilloscope permitting several ultrasonic parameters to be evaluated. No significant difference was observed in the results based on the excitation method. Fatigue damage was not able to be identified until just prior to fatigue failure although damage was observed earlier by radio-opaque x-radiography. The damage was not detected because there was a large amount of variation in the ultrasonic parameters due to reattachment of the transducers to the specimen at every measurement interval. A difference was observed in the ultrasonic velocities measured with the different frequency transducers, due to the dispersive nature of the composite material. Recent ultrasonic results monitoring non-linear second harmonic generation show promise of being far superior to conventional linear ultrasonic techniques for detection and monitoring of fatigue damage in these composites.

Summary and Conclusions

Advanced ultrasonic and acoustic microscope techniques were optimally applied to determine the origin of defects in composite materials used in aircraft and aerospace structures. Among the materials investigated were graphite-epoxy, metal matrix, and ceramic matrix composites. Included in the techniques used were air-coupled ultrasound to detect the quality of graphite-epoxy composite prepregs. A novel micro-photoelastic system was developed for measurement of residual stress in optically translucent ceramic matrix composites. Acoustic microscope C-scans were capable of detecting misplaced and misaligned fibers, fiber breaks, irregular resin distributions, porosity, voids, delaminations, and cracks.

The results of this research will serve to assist industrial manufacturers of composite structures to apply optimum nondestructive evaluation techniques for location and identification of defects in these structures during manufacture and to detect and monitor defect creation and growth during in-service life.

References

1. R.E. Green, Jr., Ultrasonic Investigation of Mechanical Properties, Vol. III, Treatise on Materials Science and Technology, Academic Press, New York (1973).

2. G.A. Matzkanin, G.L. Burkhardt, and C.M. Teller, Nondestructive Evaluation of Fiber Reinforced Epoxy Composites: A State of the Art Survey, AD AO71-973, April 1979, 198 pages.

3. M.J. Golis, R.P. Mester, J.L. Crowe, and G.J. Posakony, Investigation of Techniques to Nondestructively Test Reinforced Plastic Composite Pipe. AD 744 294, December 1973, 148 pages.

4. C.N. Owston, Carbon Fiber Reinforced Polymers and Nondestructive Testing, British Journal of NDT, 15, 2-11 (1973).

5. R.M. Collins, NDT Chronology of Advanced Composites at Grumman Aerospace, Materials Evaluation 39, 1126-1129 (1981).

6. J.L. Cook, W.W. Reinhardt, and J.E. Zimmer, Development of Non-Destructive Test Techniques for Multidirectional Fiber Reinforced Resin Matrix Composites, AD 746 592, October 1971, 186 pages.

7. D.J. Hagemaier and R.H. Fassbender, Nondestructive Testing of Advanced Composites, Materials Evaluation, pp.43-49, (June 1979).

8. D.J. Hagemaier and R.H. Fassbender, Nondestructive Testing of Advanced Composites, Douglas Aircraft Paper 6774, presented at SAE Aerospace Meeting, pp.1-9, (November 1978).

9. D. Hagemaier, H.J. McFaul, and D. Moon, Nondestructive Testing of Graphite Fiber Composite Structures, Materials Evaluation 29, 133-142.

10. E.G. Henneke and J.C. Duke, A Review of the State-of-the-Art of Nondestructive Evaluation of Advanced Composite Materials, Virginia Polytechnic Institute and State University, Department of Engineering Science and Mechanics, Blacksburg, VA (September 1979).

11. D.H. Kaelble, Quality Control and Nondestructive Evaluation Techniques for Composites - Part I: Overview of Characterization Techniques for Composite Reliability, AD A118 410, (May 1982), 79 pages.

12. J.P. Maigret and G. Jube, Advanced NDT Methods for Filament Wound Pressure Vessels and Composites in General, SAMPE, Science of Advanced Materials and Process Engineering Series, 16, 123-137 (1971).

13. George A. Matzkanin, Nondestructive Evaluation of Fiber Reinforced Composites, A State-of-the-Art Survey, Vol.1, NDE of Graphite Fiber Reinforced Plastic Composites, NTIAC 82-1, March 1982, 62 pages.

14. Sharon A. McGovern, NDI Survey of Composite Structures, AD A081801, January 1980, 66 pages.

15. R.B. Pipes (ed.), Nondestructive Evaluation and Flaw Criticality for Composite Materials, ASTM STP 696, October 1978.

16. R. Prakash, Nondestructive Testing of Composites, Composites 11, 217-224 (1980).

17. W.N. Reynolds, Nondestructive Examination of Composite Materials, A Survey of European Literature, AD A100454, AVRADCOM Report No. TR 81-F-6, May 1981, 76 pages.

18. I.G. Scott and C.M. Scala, NDI of Composite Materials, AD A106278, July 1981, 30 pages.

19. Alex Vary, A Review of Issues and Strategies in Nondestructive Evaluation of Fiber Reinforced Structural Composites, 11th National SAMPE Technical Conference, Materials and Processes for the Eighties, November 1979, pp. 166-177.

20. Nondestructive Testing, A Survey, NASA SP 5113, 1973, 282 pages.

21. R.A. Blake, Jr., Ultrasonic NDE of Composite Materials, Center for Composite Materials Report CCM-79-3, The University of Delaware, Newark, December 1979, 114 pages.

22. Albert M. Lindrose, Ultrasonic Wave and Moduli Changes in a Curing Epoxy Resin, Experimental Mechanics, 18, 227-232 (1978).

23. E.G. Henneke, W.W. Stinchcomb, and K.L. Reifsnider, Some Ultrasonic Methods for Characterizing Response of Composite Materials, NBS Special Publication 596, Ultrasonic Materials Characterization.

24. W. Hand, M. Silvergleit, and G.R. Arcus, Nondestructive Ultrasonic Examination of Epoxy Glass Reinforced, Filament Wound, Cylindrical Deep Submergence Test Models, Report 9-32 DTNSRDC, October 1970, 49 pages.

25. B.R. Jones and D.E.W. Stone, Towards an Ultrasonic-Attenuation Technique to Measure Void Content in Carbon Fibre Composites, Nondestructive Testing 9, 71-79 (1976).

26. B.G. Martin, Ultrasonic Attenuation Due to Voids in Fiber Reinforced Plastics, NDT International 9, 242-246 (1976).

27. D.E.W. Stone, Non-Destructive Inspection of Composite Material for Aircraft Structural Applications, British Journal of NDT, March 1978, pp.65-75.

28. D.E.W. Stone and B. Clark, Ultrasonic Attenuation as a Measure of Void Content in Carbon Fibre Reinforced Plastics, Non-Destructive Testing 8, 137-145 (1975).

29. W.H.M. Van Dreumel, Ultrasonic Scanning for Quality Control of Advanced Composites, NDT International 11, 233-235 (1978).

30. D.S. Forli and S. Torp, NDT of Glass Fiber Reinforced Plastics (GRP), Paper 4B2 Eighth World Conference on NDT, Cannes, France (1976).

31. R. Prakash and C.N. Owston, Ultrasonic Determination of Lay-up Order in Cross Plied CFRP, Composites 8, 100-102 (1977).

32. J.H. Williams and B. Dole, Ultrasonic Attenuation as an Indicator of Fatigue Life of Graphite/Epoxy Fiber Composites, NASA Contractor Report 3179, December 1979.

33. M. Meron, Y. Bar-Cohen, and O. Ishai, Nondestructive Evaluation of Strength Degradation in Glass-Reinforced Plastic as a Result of Environmental Effects, Journal of Testing and Evaluation, 5, 394-396 (1977).

34. Alex Vary, Quantitative Ultrasonic Evaluation of Engineering Properties in Metal, Composites and Ceramics, NASA-TM-81530, 1980, 18 pages.

35. A. Vary and K.J. Bowles, An Ultrasonic-Acoustic Technique for Nondestructive Evaluation of Fiber Composite Quality, Polymer Engineering and Science, 9, 373-376 (1979).

36. A. Vary and K.J. Bowles, Ultrasonic Evaluation on the Strength of Unidirectional Graphite/Polymide Composites, 11th Symposium on Nondestructive Evaluation, April 1977, San Antonio, TX, 26 pages.

37. A. Vary and R.F. Lark, Correlation of Fiber Composite Tensile Strength with the Ultrasonic Stress Wave Factor, Journal of Testing and Evaluation 7, 185-191 (1979).

38. Y. Bar-Cohen, E. Harnik, M. Meron, and R. Davidson, Ultrasonic Nondestructive Evaluation Method for the Detection and Identification of Defects in Filament Wound Glass Fiber-Reinforced Plastic Tubes, Materials Evaluation 37, 51-55 (1979).

39. G.P. Capsimalis, G. D'Andrea, and R. Peterson, Ultrasonic and Acoustic Holographic Techniques for Inspection of Composite Gun Tubes and Other Weapon Components, AD-A039 605, March 1977, 57 pages.

40. Y. Bar-Cohen, U. Arnon, and M. Meron, Defect Detection and Characterization in Composite Sandwich Structure by Ultrasonics, SAMPE Journal 14, 4-8 (1978).

41. T. Liber, I.M. Daniel, and S.W. Schramm, Ultrasonic Techniques for Inspecting Flat and Cylindrical Composite Specimens, ASTM STP 696,Nondestructive Evaluation and Flaw Criticality for Composite Structures, R.B. Pipes (ed.), pp.5-25, (1978).

42. S. Friedman and M. Silvergleit, The Nondestructive Evaluation of Graphite/Epoxy Composite Materials, DTNSRDC Center Report TM-28-75-248, April 1976.

43. Y. Bar-Cohen, M. Meron, and O. Ishai, Nondestructive Evaluation of Hygrothermal Effects on Fiber-Reinforced Plastic Laminates, Journal of Testing and Evaluation 7, 291-296 (1979).

44. A. Vary and K.J. Bowles, Ultrasonic Evaluation of the Strength of Unidirectional Graphite-Polyimide Composites, NASA TM-X-73646 (1977).

45. A. Vary and K.J. Bowles, Use of an Ultrasonic-Acoustic Technique for Nondestructive Evaluation of Fiber Composite Strength, NASA TM-73813 (1978).

46. A. Vary and K.J. Bowles, An Ultrasonic-Acoustic Technique for Nondestructive Evaluation of Fiber Composite Quality, Polymer Engr. & Sci. 19, 373-376 (1979).

47. A. Vary and R.F. Lark, Correlation of Fiber Composite Tensile Strength with the Ultrasonic Stress Wave Factor, NASA TM-78846 (1978).

48. A. Vary and R.F. Lark, Correlation of Fiber Composite Tensile Strength with the Ultrasonic Stress Wave Factor, J. of Testing and Evaluation 7, 185-191 (1979).

49. E.G. Henneke, II, J.C. Duke, Jr., W.W. Stinchcomb, A. Govada and A. Lemascon, A Study of the Stress Wave Factor Technique for the Characterization of Composite Materials, NASA CR 3670.

50. A. Govada and J.C. Duke, Jr., Application of Ultrasonics to Damage Development in Metal Matrix Composites, ASNT Paper Summaries, (1982) pp.379-385.

51. J.C. Duke, Jr., E.G. Henneke, II, W.W. Stinchcomb and K.L. Reifsnider, Characterization of Composite Materials by Means of the Ultrasonic Stress Wave Factor, in Composite Structures 2, I.H. Marshall (ed.), Applied Scientific Publishers, (1983) pp.53-60.

52. A.K. Govada, J.C. Duke, Jr., E.G. Henneke, II and W.W. Stinchcomb, A Study of the Stress Wave Factor Technique for the Characterization of Composite Materials, Center for Composite Materials and Structures Report CCMS-84-13, Virginia Polytechnic Institute and State University, Blacksburg, VA (1984).

53. Ruud, Clay Olaf and Green, Robert E., Jr.,(eds.), Nondestructive Methods for Material Property Determination, Plenum Press, New York (1984).

54. Green, Robert E., Jr., "Nondestructive Acoustic Testing for Fatigue Damage", McGraw-Hill Yearbook of Science & Technology 1985, McGraw-Hill Book Co., New York, pp. 291-294 (1984).

55. Prosser, W.H. and Green, R.E. Jr., "NDE of Composites Using Laser Generated Acoustic Waves", Proceedings of the 1985 Spring Conference on Experimental Mechanics, Las Vegas, Nevada (June 1985), Society for Experimental Mechanics, Brookfield Center, Connecticut, pp.340-346 (1985).

56. Green, Robert E., Jr.,"Ultrasonic Attenuation Nondestructive Evaluation of Materials", Proceedings of Eighth International Conference on Internal Friction and Ultrasonic Attenuation in Solids, Urbana, Illinois Journal de Physique 46, C10-827-C10-834 (1985).

57. Green, Robert E., Jr., "Ultrasonic Materials Characterization", Proceedings of Ultrasonics International 85 Conference, London, England, Butterworth, Guildford, England, pp.11-16 (1985).

58. Crane, Roger and Green, Robert E., Jr., "Polymers Nondestructive Evaluation" Encyclopedia of Materials Science and Engineering, M.B. Bever (ed.), M.I.T. Press, Cambridge, Massachusetts, pp. 3767-3771 (1986).

59. Green, Robert E., Jr., "Ultrasonic Nondestructive Evaluation", Encyclopedia of Materials Science and Engineering, M.B. Bever (ed.), M.I.T. Press, Cambridge, Massachusetts, pp. 5178-5182 (1986).

60. Green, Robert E., Jr., "Ultrasonic Nondestructive Materials Characterization", Proceedings of Analytical Ultrasonics in Materials Research and Testing Conference, NASA Lewis Research Center, Cleveland, Ohio pp. 1-30 (1986).

61. Green, Robert E., Jr., "Ultrasonic Methods", Proceedings of Third Advanced Materials Workshop, Michigan State University, Traverse City, Michigan, September (1986).

62. Bussiere, Jean F., Monchalin, Jean-Pierre, Ruud, Clay Olaf and Green, Robert E., Jr.,(Editors), Nondestructive Material Property Characterization, Plenum Press, New York (1987).

63. Prosser, William H. and Green, Robert E., Jr., "Ultrasonic Characterization of the Nonlinear Elastic Properties of Graphite/Epoxy Composites", Proceedings of Ultrasonic International 87 Conference, pp. 172-177, Butterworth Scientific Ltd., Guilford, Surrey, England (1987).

64. Prosser, William H. and Green, Robert E., Jr., "Ultrasonic Measurement of the Nonlinear Elastic Properties of Graphite/Epoxy Composites for Applications Toward Nondestructive Evaluation", Proceedings of 1987 Society of Engineering Science Annual Meeting, Salt Lake City, Utah, September 1987.

65. Prosser, William H. and Green, Robert E., Jr., "Characterization of the Nonlinear Elastic Properties of Graphite/Epoxy Composites Using Ultrasound", Proceedings of American Society for Composites/University of Delaware Center for Composite Materials Joint Symposium on Composite Materials Science and Engineering, pp. 123-132, University of Delaware, Newark, (1987).

66. Green, Robert E., Jr., "Nondestructive Characterization of Materials Properties", Mechanical Engineering, pp. 66-70 (September, 1987).

67. Wagner, James W. and Green, Robert E., Jr., "Interferometric and Holographic Testing of Composite Materials", in Quality and Damage Control in Composite Materials, A.R. Bunsell (Editor), Elsevier Applied Science Publishers, London.

68. Wagner, James W. and Green, Robert E., Jr., "Laser Generation and Detection of Ultrasound with Application to Acousto-Ultrasonics Testing of Aerospace Structures", in Proceedings of Conference on Nondestructive Evaluation for Aerospace Requirements, Huntsville, Alabama, August 1987.

69. Green, Robert E., Jr., "Advanced NDI/E Methods and Equipment for Damage Detection and Characterization and Manufacturing Control of Composite Materials and Components", in Proceedings of the Balanced Technology Initiative Conference on Advanced Materials for Conventional Defense Applications, Institute for Defense Analysis, Alexandria, Virginia, pp. 156-160 1988.

70. Wagner, James W., Green, Robert E., Jr., and Ehrlich, Michael J., "Combined Optical and Acoustic Methods for Inspection of Composite Materials", in Materials Processes: The Intercept Point, Proceedings of the 20th International SAMPE Technical Conference, Minneapolis, MN, Vol. 20, pp. 490-504 (1988).

71. Nondestructive Characterization of Materials, Proceedings of 3rd International Symposium on Nondestructive Characterization of Materials, P. Holler, V. Hauk, G. Dobmann, C.O. Ruud, and R.E. Green (Eds.), Springer Verlag, New York, (1989).

72. Green, Robert E., Jr., "Nondestructive Evaluation for Materials Characterization", in Non-Destructive Monitoring of Materials Properties, J. Holbrook and J. Bussiere (Eds.), Material Research Society, Pittsburgh, PA, Vol. 142, pp. 15-25 (1989).

73. Green, Robert, E., Jr., "Nondestructive Evaluation Techniques in Materials Science", in New Materials and Processes, I.L.H. Hansson and H. Lilholt (Eds.), Proceedings of the 5th Scandinavian Symposium on Materials Science, Danish Society for Materials Testing and Research, Ingenhiorhuset, Copenhagen, Denmark, pp. 1-16, (1989).

74. Green, Robert, E., Jr., "Nondestructive Characterization of Materials", Advanced Materials & Processes, ASM International, Metals Park, Ohio, 136, 20-22 (1989).

75. Prosser, William H. and Green, Robert E., Jr., "Characterization of the Nonlinear Elastic Properties of Graphite/Epoxy Composites Using Ultrasound", Journal of Reinforced Plastics and Composites, 9, 162-173 (1990).

76. Krynicki, J.W., Green, R.E., Jr. and Nagle, D.C., "Acoustic Emission of Discrete Failure Modes in Ceramic/Ceramic Composites", Proceedings of the Conference on Nondestructive Evaluation of Modern Ceramics, Columbus, OH pp. 144-149 (1990).

77. Green, R.E., Jr., Nondestructive Evaluation of Materials, Annual Review of Materials Science 20, 197-217 (1990).

78. Krynicki, J.W., Nagle, D.C., and Green, R.E., Jr., "Direct Thermomechanical Stress and Failure Mode Analysis of a Cloth Reinforced Ceramic Matrix Composite", Nondestructive Material Property Characterization, Proceedings of the Fourth International Symposium on Nondestructive Characterization of Materials, Annapolis, MD (1990), Plenum Press, New York (1991).

79. Ruud, Clay Olaf, Green, Robert E., Jr., and Bussiere, Jean F., (Editors), Nondestructive Material Property Characterization, Proceedings of the Fourth International Symposium on Nondestructive Characterization of Materials", Annapolis, MD Plenum Press, New York (1991).

80. Krynicki, J.W., Green, R.E., Jr., and Nagle, D.C., "Discrete Failure Mode Detection in a Woven SiC Cloth Reinforced Glass Composite", J. Materials Science 26, 2184-2188 (1991).

81. Krynicki, J.W., Green, R.E., Jr., and Nagle, D.C., "Quantifying Processing Stresses in Composites", Review of Progress in Quantitative Nondestructive Evaluation", 11B, 1507-1514, Plenum Press (1991).

82. Green, R.E., Jr., and Krynicki, J.W., "Recent Advances in Nondestructive Evaluation of Ceramic/Ceramic Composites", Keynote Invited Lecture, Proceedings of Second European Ceramic Society Conference, Augsburg, Germany, (1991).

83. Gianaris, N.J. and Green, R.E., Jr., "Acoustic Emission, Infrared Thermography, and Ultrasonic Attenuation Monitoring of Fatigue Damage in Thick Composite Materials in Compression", Nondestructive Evaluation and Material Properties of Advanced Materials, P.K. Liaw et al. (Eds.), TMS, Warrendale, PA pp. 29-35 (1991).

84. Green, R.E., Jr., "Overview of Acoustical Technology for Nondestructive Evaluation", Proceedings of Second International Congress on Recent Developments in Air- and Structure-Borne Sound and Vibration", M.J. Crocker & P.K. Raju (Eds.), Vol 2, pp. 879-886 (1992).

85. R.E. Green, Jr., "Special Problems Associated with Ultra sonic Wave Propagation in Anisotropic Materials", in Nondestructive Characterization of Materials V, T. Kishi et al. (Eds.), Iketani Science & Technology Foundation, Tokyo, Japan, pp. 469- 476 (1992).

86. T. Kishi, T. Saito, C. Ruud, & R.E. Green, Jr., (Eds.) Nondestructive Characterization of Materials V, Iketani Science & Technology Foundation, Tokyo, Japan (1992).

87. Xia Teng, Xuan Kong, and Robert E. Green, Jr., "Ultrasonic Tomography of Anisotropic Materials", Proceedings 1992 JANNAF Nondestructive Evaluation Subcommittee Meeting, Seattle, WA, CPIA Publication 584, pp. 1-11 (1992)

88. Green, R.E., Jr., "Practical Applications of Nondestructive Materials Characterization", J. Minerals, Metals & Materials, **44**, 12-16 (1992).

89. Krynicki, J.W., Nagle, D.C., and Green. R.E., Jr., "Photoelastic Measurement of Residual Thermomechanical Stress in SiC-Reinforced Glass Composites", J. Am. Ceram. Soc. **75**, 2225-2231 (1992).

90. Green, R.E., Jr., "Nondestructive Evaluation of Ceramics", Proceedings of the International Ceramics Conference, Melbourne, Australia, M.J. Bannister (Ed.), Vol. 1, pp.377-386 (1992).

91. Teng, X., Boltz, E. and Green, R.E., "Ultrasonic Tomography of Anisotropic Materials", Proceedings of 14th International Congress on Acoustics, Beijing, China, Vol. 2, Paper C15-1 (1992).

92. Teng, X. and Green, R.E., "Ultrasonic Tomographic Imaging of Defects in Industrial Materials", Review of Progress in Quantitative NDE, Vol. 12B, pp. 889-896 (1993)

93. Boltz, E.S. and Green, R.E., "Ultrasonics in Thick Anisotropic Materials", Review of Progress in Quantitative NDE, Vol. 12B, pp. 1241-1248 (1993).

94. Byrne, C., Krynicki J.W., and Green, R.E., "Damage Accumulation in Graphite-Epoxy Composites During Compressive Fatigue", Review of Progress in Quantitative NDE, Vol. 12B, pp. 1369-1396 (1993).

95. Byrne, C. and Green, R.E., "Damage Accumulation in Thick Composites During Compressive Fatigue", Proceedings of Society for Experimental Mechanics Fall Meeting, Chicago, IL (1993).

96. Green, R.E. and Byrne, C. "Nondestructive Detection of Compressive Fatigue Damage in Thick Composites" Proceedings of Society for Experimental Mechanics Fall Meeting, Chicago, IL (1993).

97. Byrne, C., and Green, R.E., Jr., "Acoustic Emission Monitoring of Thick Composite Laminates Under Compressive Loads", Nondestructive Characterization of Materials VI, R.E. Green, Jr., C.O. Ruud, and M. Manghnani (Eds.), Plenum, New York (1994).

98. Gavens, A.J., and Green, R.E., Jr., "Ultrasonic Evaluation of Composite Fatigue Damage", Nondestructive Characterization of Materials VI, R.E. Green, Jr., K.J. Kozaczek, and C.O. Ruud (Eds.), Plenum Publishing Corp., New York (1994).

99. Nondestructive Characterization of Materials VI, R.E. Green, Jr., K.J. Kozaczek, and C.O. Ruud (Eds.), Plenum Publishing Corp., New York (1994).